MATCH
Communications in Mathematical and in Computer Chemistry

MATCH Commun. Math. Comput. Chem. **79** (2018) 215-260

ISSN 0340 - 6253

A New High Order Method with Optimal Stability and Phase Properties

Maxim A. Medvedev[a, b], **Theodore E. Simos**[1a, c,d]

[a] *Group of Modern Computational Methods, Ural Federal University, 620002, 19 Mira Street, Ekaterinburg, Russian Federation*

[b] *Institute of Industrial Ecology UB RAS Sophy Kovalevskoy 20, Yekaterinburg Russian Federation 620990*

[c] *Data Recovery Key Laboratory of Sichuan Province, College of Mathematics and Information Science, Neijiang Normal University, Neijiang 641100, PR China*

[d] *Laboratory of Computational Sciences, Department of Informatics and Telecommunications, Faculty of Economy, Management and Informatics, University of Peloponnese, GR-221 00 Tripolis, Greece (Part Time)*
tsimos.conf@gmail.com

(Received May 25, 2017)

Abstract

In the present paper we develop, for the first time in the literature, a high algebraic order P–stable symmetric two–step method with eliminated phase–lag and its derivatives up to order three. The development of the new scheme is based on the following procedure: (1) The necessary and sufficient conditions for P–stability are satisfied. (2) The condition of the elimination of the phase–lag is also satisfied and finally (3) The conditions of the elimination of the derivatives of the phase–lag up to order three are also satisfied.

Based on the above the coefficients of the method is determined.

The result of the above described procedure is the construction, for the first time in the literature, of a three–stages P–stable tenth algebraic order symmetric two–step method with vanished phase–lag and its first, second and third derivatives.

The following investigation is also presented, for the new obtained method:

[1] Highly Cited Researcher, Active Member of the European Academy of Sciences and Arts Active Member of the European Academy of Sciences Corresponding Member of European Academy of Arts, Sciences and Humanities

1. the construction of the scheme (based on the above procedure of three stages),
2. the computation of its local truncation error (LTE),
3. the determination of the asymptotic form of the LTE, which will be based on the radial Schrödinger equation,
4. the stability analysis of the computation of the stability domain and the interval of periodicity,
5. the determination of the embedded pair for the LTE control procedure and the definition the change of the stepsize of the integration and determination of the variable step procedure,
6. the evaluation of the computational effectiveness of the new obtained pair with application on: (i) the resonance problem of the radial Schrödinger equation and on (ii) the coupled differential equations arising form the Schrödinger equation.

The above achievements leads to the conclusion that the new obtained P-stable high algebraic order scheme with vanished phase–lag and its derivatives up to order three is more efficient methods than the existed ones.

1 Introduction

In this paper and for the first time in the literature we develop a new three stages P–stable symmetric two–step method with vanished phase–lag and its derivatives up to order three. The development of the new pair is based on the following steps:

- Satisfaction of the conditions for the P–stability.
- Satisfaction of the conditions for the vanishing of the phase–lag.
- Satisfaction of the conditions for the vanishing of the derivatives of the phase–lag up to order three.

The efficiency of the new obtained numerical pair is examined via application to the following problems:

- the radial time independent Schrödinger equation and
- the coupled Schrödinger equations.

The effective solution of the above mentioned problems is critical in Computational Chemistry (see [7] and references therein) since an important part of the quantum chemical computations contains the Schrödinger equation (see [7] and references therein). We

mention also that in problems with more than one particle the numerical solution of the Schrödinger's equation is necessary. The efficient numerical solution of the Schrödinger's equation gives us the following important information:

- numerical computations of molecular properties (vibrational energy levels and wave functions of systems) and
- numerical presentation of the electronic structure of the molecule (see for more details in [8–11]).

An embedded numerical pair is presented also in this paper which is based on an error control procedure and a variable–step scheme.

The problems studied in this paper belong to the special category of problems with the general form:

$$q''(x) = f(x,q), \;\; q(x_0) = q_0 \;\; and \;\; q'(x_0) = q'_0. \tag{1}$$

with periodical and/or oscillating solutions

The large research which has been done on the general subject of this paper and its bibliography can be categorized into the following categories:

- Exponentially, trigonometrically and phase fitted Runge–Kutta and Runge–Kutta Nyström methods: [45], [48], [57], [60] – [65], [54] [76]. In this category of methods, Runge–Kutta and Runge–Kutta Nyström schemes are obtained. We can divide this category into two subcategories:
  - The numerical pairs have the property of exact integration of functions of the form:

$$x^i \cos(\omega x), \; i = 0,1,2,\ldots \text{or} \;\; x^i \sin(\omega x), \; i = 0,1,2,\ldots$$
$$\text{or} \;\; x^i \exp(\omega x), \; i = 0,1,2,\ldots \tag{2}$$

    or combination of the above functions.
  - The numerical pairs have the property of vanishing of the phase–lag.

We note here that ω denotes the frequency of the problem.

- Multistep exponentially, trigonometrically and phase fitted methods and multistep methods with minimal phase–lag: [1]– [4], [16]– [19], [23]– [26], [32], [36], [38], [42], [46]– [47], [51], [56], [58]– [59], [69]– [71], [77]– [80]. In this category of methods, multistep schemes are developed. We can divide this category into two subcategories:
  - The multistep pairs have the property of exact integration of functions of the form (2) or combination of the functions of the form (2).
  - The multistep pairs have the property of vanishing of the phase–lag.

  We note here that ω denotes the frequency of the problem.
- Symplectic integrators: [40]– [41], [49], [52], [55], [65]– [68], [74]. In this category of numerical pairs, algorithms for which the Hamiltonian energy of the system remains almost constant during the integration procedure, are obtained.
- Nonlinear methods: [50]. In this category of numerical pairs, schemes have nonlinear form (i.e. the relation betweens several approximations of the function in several points of the integration domain y_{n+j}, $j = 0, 1, 2, \ldots$ is nonlinear) are obtained.
- General methods: [12]– [15], [20]– [22], [33]– [35], [39]. In the category of numerical pairs, algorithms with constant coefficients are produced.

2 General theory for the symmetric multistep method

The general theory of the symmetric multistep methods is described in this section. We focus on this theory since the methods which we study in this paper belong to this category.

Using the methodology of discretization of the integration area $[a, b]$, we can numerically solve problems of the general form (1) using the $2\,m$-step method presented below (3). In this case the parameter m denotes the number of the discretization points.

The following symbols will be used in this paper:

- h is stepsize of the integration which is the same with the step length of the discretization. It is denoted as $h = |x_{i+1} - x_i|$, $i = 1 - m(1)m - 1$ (i.e. the i is moved between $1 - m$ and $m - 1$ with step 1) where

- x_n represents the n-th point on the discretized area.
- q_n represents the approximated value of the function $q(x)$ at the point x_n. The approximated value is computed using a numerical pair and in our study the numerical pair which is used is the $2\,m$-step method (3) presented below

We consider the family of $2\,m$-step methods which they have the following general form:

$$\Delta\,(m) : \sum_{i=-m}^{m} \alpha_i\, q_{n+i} = h^2 \sum_{i=-m}^{m} \beta_i\, f(x_{n+i}, q_{n+i}) \tag{3}$$

for the numerical solution of the initial value problem (1) on the in integration domain $[a, b]$. We note that α_i and β_i $i = -m(1)m$ are the coefficients of the $2\,m$-step method.

Definition 1.

$$\Delta\,(m) \rightarrow \begin{cases} \beta_m \neq 0 & \textit{implicit;} \\ \beta_m = 0 & \textit{explicit.} \end{cases} \tag{4}$$

Definition 2.

$$\Delta\,(m) \;\; \textit{with } \alpha_{i-m} = \alpha_{m-i},\, \beta_{i-m} = \beta_{m-i},\, i = 0(1)m \rightarrow \textit{symmetric} \tag{5}$$

Remark 1. *We note that the method $\Delta\,(m)$ is associated with the linear operator*

$$L(x) = \sum_{i=-m}^{m} \alpha_i\, q(x + i\,h) - h^2 \sum_{i=-m}^{m} \beta_i\, q''(x + ih) \tag{6}$$

where $q \in \mathbb{C}^2$ (i.e. $\mathbb{C}^2 \equiv \mathbb{C}x\mathbb{C}$).

Definition 3. *[12] The corresponding multistep method (3) is called of algebraic order p, if the linear operator L (6) eliminates for any linear combination of the linearly independent functions $1,\, x,\, x^2,\, \ldots,\, x^{p+1}$.*

If we apply a symmetric $2\,m$-step method $\Delta\,(m)$ to the test problem

$$q'' = -\phi^2\, q \tag{7}$$

then we obtain the difference equation:

$$\Upsilon_m(v)\, q_{n+m} + ... + \Upsilon_1(v)\, q_{n+1} + \Upsilon_0(v)\, q_n$$
$$+\Upsilon_1(v)\, q_{n-1} + ... + \Upsilon_m(v)\, q_{n-m} = 0 \tag{8}$$

and its associated characteristic equation:

$$\Upsilon_m(v)\, \lambda^m + ... + \Upsilon_1(v)\, \lambda + \Upsilon_0(v)$$
$$+\Upsilon_1(v)\, \lambda^{-1} + ... + \Upsilon_m(v)\, \lambda^{-m} = 0. \tag{9}$$

where

- $v = \phi\, h$,
- h is the stepsize or step length of the integration and
- $A_j(v)$, $j = 0(1)m$ are the stability polynomials.

Definition 4. [13] *A symmetric $2\,m$-step method is called that has an non zero interval of periodicity $(0, v_0^2)$, if its characteristic equation (9), for all $v \in (0, v_0^2)$, has the following roots :*

$$\lambda_1 = e^{i\psi(v)},\ \lambda_2 = e^{-i\psi(v)},\ \text{and } |\lambda_{\mathrm{i}}| \leq 1,\ \mathrm{i} = 3(1)2\,\mathrm{m} \tag{10}$$

where $\psi(v)$ is a real function of v.

Definition 5. *(see [13]) A symmetric multistep method is called P-stable it its interval of periodicity is equal to $(0, \infty)$.*

Remark 2. *A symmetric multistep method considered as P-stable if the following necessary and sufficient conditions are hold:*

$$|\lambda_1| = |\lambda_2| = 1 \tag{11}$$
$$|\lambda_j| \leq 1, j = 3(1)2m,\ \forall v. \tag{12}$$

Definition 6. *A symmetric multistep method is called singularly P-stable if its interval of periodicity is equal to $(0, \infty)\backslash S$ with S a finite set of points.*

Definition 7. [14], [15] *The symmetric multistep method with associated characteristic equation given by (9), has phase-lag which is defined as the leading term in the expansion of*

$$t = v - \psi(v). \tag{13}$$

If $t = O(v^{t+1})$ as $v \to \infty$ then we call that the phase-lag order is equal to t.

Definition 8. *[16] A symmetric multistep method is called* **phase-fitted** *if it has phase-lag equal to zero.*

Theorem 1. [14] *For a symmetric $2\,m$-step method with characteristic equation given by (9) a direct formula for the computation of the phase-lag order t and the phase-lag constant c is given by*

$$-cv^{t+2} + O(v^{t+4}) = \frac{2\,\Upsilon_m(v)\,\cos(m\,v) + ... + 2\,\Upsilon_j(v)\,\cos(j\,v) + ... + \Upsilon_0(v)}{2\,m^2\,\Upsilon_m(v) + ... + 2\,j^2\,\Upsilon_j(v) + ... + 2\,\Upsilon_1(v)} \tag{14}$$

Remark 3. *For the symmetric two–step methods the phase-lag order t and the phase-lag constant c are computed using the formula:*

$$-cv^{t+2} + O(v^{t+4}) = \frac{2\,\Upsilon_1(v)\,\cos(v) + \Upsilon_0(v)}{2\,\Upsilon_1(v)} \tag{15}$$

assuming that their stability polynomials are equal to $\Upsilon_j(v)\; j = 0, 1,$

3 A P–stable three–stages symmetric two–step method with vanished phase–lag and its first, second and third derivatives

We We consider the following family of methods

$$\begin{aligned}
\widehat{q}_{n+1} &= q_{n+1} - h^2\left(c_1\,f_{n+1} - c_0\,f_n + c_1\,f_{n-1}\right)\\
\tilde{q}_{n+1} &= q_{n+1} - h^2\left(c_3\,\widehat{f}_{n+1} - c_2\,f_n + c_3\,f_{n-1}\right)\\
q_{n+1} + a_1\,q_n + q_{n-1} &= h^2\left[b_1\,\left(\tilde{f}_{n+1} + f_{n-1}\right) + b_0\,f_n\right]
\end{aligned} \tag{16}$$

where $f_{n+i} = q''\left(x_{n+i}, q_{n+i}\right), i = -1(1)1,\ \widehat{f}_{n+1} = q''\left(x_{n+1}, \widehat{q}_{n+1}\right),\ \tilde{f}_{n+1} = q''\left(x_{n+1}, \tilde{q}_{n+1}\right)$ and a_1, b_i, $i = 0, 1$ and c_j, $i = 0\,(1)\,3$ are parameters.

Remark 4. *We observe that the new scheme has three stages. All the stages of the new pair are based on the approximation on the point x_{n+1}.*

We investigate the case:

$$b_0 = \frac{5}{6},\ b_1 = \frac{1}{12},\ c_3 = \frac{1}{30}. \tag{17}$$

Remark 5. *The above constant values of the coefficients of the family of methods (16) are denoted requiring the pair to have the maximum possible algebraic order.*

Applying the pair (16) with the constant coefficients given by (17) to the test problem (7) we obtain the difference equation (8) with $m = 1$ and the corresponding characteristic equation (9) with $m = 1$ where:

$$\Upsilon_0(v) = 1 + \frac{1}{12}v^2 + \frac{1}{360}v^4 + \frac{1}{360}v^6 c_1 \tag{18}$$

$$\Upsilon_1(v) = a_1 + \frac{5}{6}v^2 - \frac{1}{12}v^4 c_2 - \frac{1}{360}v^6 c_0 \tag{19}$$

The development of the new pair is based on the flowchart of Figure 1 (for developing flowcharts in LaTeX one can see [88]):

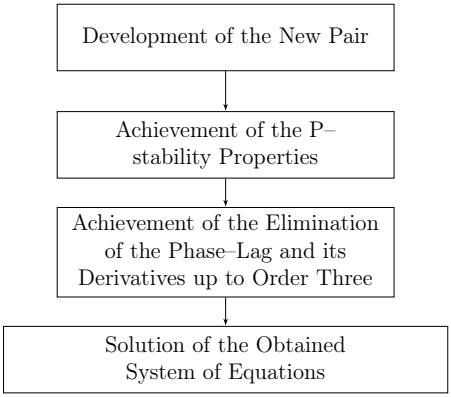

Figure 1. Flowchart for the development of the new scheme of P–stable three stages symmetric two–step methods with vanished phase–lag and its derivatives up to order three

3.1 First step of the construction of the new pair achievement the P–stability properties

In order to achieve the P–stability properties we follow the methodology first introduced by Lambert and Watson [13] and Wang [81]:

- The satisfaction of the characteristic equation given by (9) with $m = 1$ for $\lambda = e^{I\,v}$, where $I = \sqrt{-1}$ which leads to the following equation:

$$\left(\mathrm{e}^{I\,v}\right)^2\,\Upsilon_0\left(v\right) + \mathrm{e}^{I\,v}\,\Upsilon_1\left(v\right) + \Upsilon_0\left(v\right) = 0 \tag{20}$$

- The satisfaction of characteristic equation given by (9) with $m = 1$ for $\lambda = e^{-I\,v}$, where $I = \sqrt{-1}$ which leads to the following equation:

$$\left(\mathrm{e}^{-I\,v}\right)^2\,\Upsilon_0\left(v\right) + \mathrm{e}^{-I\,v}\,\Upsilon_1\left(v\right) + \Upsilon_0\left(v\right) = 0 \tag{21}$$

The above mentioned conditions are produced based on the Definition 4 taking into account that the new proposed pair has the characteristic equation given by (9) with $m = 1$.

3.2 Second stage of the construction of the new pair achievement of elimination of the phase–lag of the pair and its derivatives up to order three

In order to achieve the elimination of the phase–lag and its derivatives up to order three for the above scheme (16) with the coefficients given by (17), the following system of equations is hold:

$$\mathrm{Phase}-\mathrm{Lag(PL)}\;=\;\frac{1}{2}\,\frac{\Upsilon_2\left(v\right)}{v^6c_1+v^4+30\,v^2+360} = 0 \tag{22}$$

$$\mathrm{First\,Derivative\,of\,the\,Phase}-\mathrm{Lag}\;=\;\frac{\Upsilon_3\left(v\right)}{\left(v^6c_1+v^4+30\,v^2+360\right)^2} = 0 \tag{23}$$

$$\mathrm{Second\,Derivative\,of\,the\,Phase}-\mathrm{Lag}\;=\;\frac{\Upsilon_4\left(v\right)}{\left(v^6c_1+v^4+30\,v^2+360\right)^3} = 0 \tag{24}$$

$$\mathrm{Third\,Derivative\,of\,the\,Phase}-\mathrm{Lag}\;=\;\frac{\Upsilon_5\left(v\right)}{\left(v^6c_1+v^4+30\,v^2+360\right)^4} = 0 \tag{25}$$

where $\Upsilon_j\left(v\right),\ j = 2(1)5$ are given in the Appendix A.

3.3 Final stage of the construction of the new pair solution of the obtained system of equations

The solution of the system of equations (20), (21), (22)–(25) leads to the determination of the the rest of the coefficients of the new pair (16):

$$a_1\;=\;\frac{\Upsilon_6\left(v\right)}{2160\,\sin\left(v\right)v^2-23760\,\cos\left(v\right)v-45360\,\sin\left(v\right)}$$

$$
\begin{aligned}
c_0 &= \frac{1}{3}\,\frac{\Upsilon_7(v)}{v^6\left(\sin(v)\,v^2-11\,\cos(v)\,v-21\,\sin(v)\right)}\\
c_1 &= -\frac{\Upsilon_8(v)}{v^6\left(\sin(v)\,v^2-11\,\cos(v)\,v-21\,\sin(v)\right)}\\
c_2 &= -\frac{\Upsilon_9(v)}{60\,v^3\left(\sin(v)\,v^2-11\,\cos(v)\,v-21\,\sin(v)\right)}
\end{aligned}
\tag{26}
$$

where $\Upsilon_j(v)$, $j = 6(1)9$ are given in the Appendix B.

During computations there is the possibility of cancellations or impossibility of definitions of the determined coefficients (26) (an example of a cancellation is the following case: the denominators of the determined coefficients lead to zero for some values of $|v|$). For these cases we give, in the Appendix C, the truncated Taylor series expansions of the determined coefficients obtained in (26).

In Figure 2 we present the behavior of the coefficients.

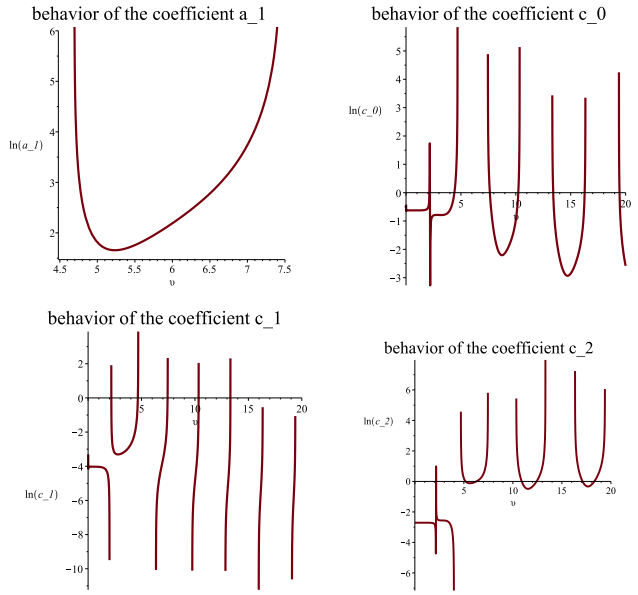

Figure 2. Behavior of the coefficients of the new proposed pair (16) given by (26) for several values of $v = \phi\,h$.

In order to complete the development of the new algorithm, we calculate the formula of its local truncation error (LTE), which is indicated as $NM3SPS3DV$ - Explanation of the abbreviation $NM3SPS3DV$ is: New Algorithm of Three–Stages P–Stable with eliminated phase–lag and its first three Derivatives, is given by:

$$LTE_{NM3SPS3DV} = -\frac{1}{23950080}\, h^{12} \left(q_n^{(12)} - 9\,\phi^4\, q_n^{(8)} \right.$$
$$\left. -16\,\phi^6\, q_n^{(6)} - 9\,\phi^8\, q_n^{(4)} + \phi^{12}\, q_n \right) + O\left(h^{14}\right). \tag{27}$$

The determination of the formula of the local truncation error (27) is important for the definition of the algebraic order of the algorithm. The form of the formula of the LTE is important in the determination of the asymptotic form of the local truncation error which is important for the error analysis which is presented below.

4 Error and stability analysis of the new proposed pair

4.1 Comparative local truncation error analysis

The local truncation error of some schemes of similar form In this section is studied in this section. For this investigation we use as test problem the radial Schrödinger equation with potential $V(x)$ which is given by:

$$q''(x) \;=\; (V(x) - V_c + \Gamma)\; q(x) \tag{28}$$

where

- $V(x)$ denotes the potential function,
- V_c denotes a constant approximation of the potential on the specific point x,
- $\Gamma = V_c - E$
- $\Xi(x) = V(x) - V_c$ and
- E denotes the energy.

The methods under evaluation are:

4.1.1 Classical method (i.e., method (16) with constant coefficients)

$$LTE_{CL} = -\frac{1}{23950080}\, h^{12}\, z_n^{(12)} + O\left(h^{14}\right). \tag{29}$$

4.1.2 P–stable linear six–step method of Wang [81]

$$LTE_{WANGPSL6S} = -\frac{81}{44800}\, h^{10} \left(z_n^{(10)} + 10\, \phi^{10}\, z_n \right) + O\left(h^{12}\right). \tag{30}$$

4.1.3 P–stable method with vanished phase–lag and its first and second derivatives developed in [6]

$$LTE_{NM3SPS2DV} = -\frac{1}{47900160}\, h^{12} \left(2\, z_n^{(12)} - 9\, \phi^4\, z_n^{(8)} \right.$$
$$\left. -8\, \phi^6\, z_n^{(6)} - \phi^{12}\, z_n \right) + O\left(h^{14}\right). \tag{31}$$

4.1.4 P–stable scheme with vanished phase–lag and its first, second and third derivatives developed in section 3

The formula of the Local Truncation Error for this method is given by (27)

The comparative error analysis is based on the following steps:

- For the pairs mentioned above with local truncation error (LTE) formulae given by (29), (30), (31) and (27) we obtain new expressions for the LTE formuale which are based on the test problem (28) which is the radial time independent Schrödinger equation. In order to achieve the new expressions of the LTE formulae given by (29), (30), (31) and (27), we have to substitute the derivatives of the function q with the formulae of the derivatives of the function q which are produced based on the the test problem (28). We present some expressions of the derivatives of the function q in the Appendix D.

- We obtain the new formulae of LTE for the above mentioned methods, based on the above step. These new formulae contain the parameter Γ and the energy E.

  The general form of the new formulae for LTE is given by:

$$LTE = h^p \sum_{j=0}^{k} K_j\, \Gamma^j \tag{32}$$

  with K_j are: 1) constant numbers (frequency independent cases i.e. the classical case) or 2) formulae of v and Γ (frequency dependent cases), p is the algebraic order of the specific method and k is the maximum possible power of Γ in the formulae of LTE.

Investigating the possible cases for the quantity Γ we arrived to the following conclusion:

- For the parameter Γ we have two cases:

  1. **The Potential is closed to the Energy.**

     Consequently:

     $$\Gamma \approx 0 \Rightarrow \Gamma^i \approx 0,\ i = 1, 2, \ldots. \tag{33}$$

     which leads to the form for the formula (32:

     Remark 6.

     $$LTE_{\Gamma=0} = h^k \Lambda_0 \tag{34}$$

     It is noted that Λ_0 is the same for all the methods of the same family, i.e. $LTE_{CL} = LTE_{NM3SPS2DV} = LTE_{NM3SPS3DV} = h^{12} \Lambda_0$, where Λ_0 is given in the Appendix E.

     Theorem 2. *Based on the formula (33) we conclude that for $\Gamma = V_c - E \approx 0$ the local truncation error for the classical method (constant coefficients - (29)), the local truncation error for the method with eliminated phase–lag and its first and second derivatives developed in [6] (with LTE given by (31) and the local truncation error for the method with eliminated phase–lag and its first, second and third derivatives developed in Section 3 (with LTE given by (27) are the same and equal to $h^{12} \Lambda_0$, where Λ_0 is given in the Appendix E.*

  2. **The Energy and the Potential are far from each other.** Consequently, $\Gamma >> 0 \vee \Gamma << 0 \Rightarrow |\Gamma| >> 0$. Therefore, the most accurate scheme is the scheme with asymptotic form of LTE which contains the minimum power of Γ and the maximum value of p in (32).

- The above achievements lead to the following asymptotic expressions of the LTE formulae for the schemes which are under evaluation.

4.1.5 Classical method

The Classical Method is the method (16) with constant coefficients.

$$LTE_{CL} = -\frac{1}{23950080}\, h^{12} \left(q\left(x\right)\, \Gamma^{6} + \cdots \right) + O\left(h^{14}\right). \tag{35}$$

We present here the leading term in the asymptotic form of the Local Truncation Error. Consequently, the symbol $\cdots$ means that there are also terms for $\Gamma^{j}\; j = 0\left(1\right) 5$.

4.1.6 P–stable linear six–step method of Wang [81]

This is the method presented in Linear Six–step Method presented in [81] (see in [81] equations (23)-(27). We note also here that there is a missprint in the paper [81]. In formula (25) $2\, C_{3,0}\, y''_{k+2}$ must be replaced by the correct: $2\, C_{3,0}\, y''_{k+3}$.

$$LTE_{WANGPSL6S} = -\frac{81}{8960}\, h^{10} \left(\Xi\left(x\right)\, q\left(x\right)\, \Gamma^{4} + \cdots \right) + O\left(h^{12}\right). \tag{36}$$

We present here the leading term in the asymptotic form of the Local Truncation Error. Consequently, the symbol $\cdots$ means that there are also terms for $\Gamma^{j}\; j = 0\left(1\right) 3$.

4.1.7 P–stable method with vanished phase–lag and its first and second derivatives developed in [6]

This is the P–stable method which we developed in [6].

$$\begin{aligned} LTE_{NM3SPS2DV} &= -\frac{1}{997920}\, h^{12} \left(\frac{\mathrm{d}^{4}}{\mathrm{d}x^{4}} \Xi\left(x\right) q\left(x\right)\, \Gamma^{4} \right. \\ &\left. + \cdots \right) + O\left(h^{14}\right). \end{aligned} \tag{37}$$

We present here the leading term in the asymptotic form of the Local Truncation Error. Consequently, the symbol $\cdots$ means that there are also terms for $\Gamma^{j}\; j = 0\left(1\right) 3$.

4.1.8 P–stable scheme with vanished phase–lag and its first, second and third derivatives developed in section 3

This is the P–stable method which we developed in Section 3.

$$\begin{aligned} LTE_{NM3SPS3DV} = -\frac{1}{997920}\, h^{12} \left[\left[4\, \Xi\left(x\right)\, q\left(x\right) \frac{\mathrm{d}^{2}}{\mathrm{d}x^{2}} \Xi\left(x\right) + 7\, q\left(x\right)\, \frac{\mathrm{d}^{4}}{\mathrm{d}x^{4}} \Xi\left(x\right) \right. \right. \\ \left. \left. + 2\, \frac{\mathrm{d}^{3}}{\mathrm{d}x^{3}} \Xi\left(x\right) \frac{\mathrm{d}}{\mathrm{d}x} q\left(x\right) + 3\, q\left(x\right)\, \left(\frac{\mathrm{d}}{\mathrm{d}x} \Xi\left(x\right) \right)^{2} \right] \Gamma^{3} + \cdots \right] + O\left(h^{14}\right). \end{aligned} \tag{38}$$

We present here the leading term in the asymptotic form of the Local Truncation Error. Consequently, the symbol $\cdots$ means that there are also terms for $\Gamma^j \; j = 0\,(1)\,2$.

The above analysis leads to the following theorem:

Theorem 3.

- *Classical Method (i.e., the method (16) with constant coefficients): For this method the error increases as the sixth power of* Γ.
- *P–stable Linear Six–step Method of Wang [81]: For this method the error increases as the fourth power of* Γ.
- *P–Stable Tenth Algebraic Order Method with Vanished Phase–Lag and Its First and Second Derivatives Developed in [6]: For this method the error increases as the fourth power of* Γ.
- *P–Stable Tenth Algebraic Order Method with Vanished Phase–Lag and Its First, Second and Third Derivatives Developed in Section 3: For this method the error increases as the third power of* Γ.

Consequently, for the approximate solution of the time independent radial Schrödinger equation, on which our analysis was based, the new P–stable tenth algebraic order method with vanished phase–lag and its derivatives up to order three is the most accurate one since it satisfies the two necessary conditions of the most accurate method i.e. (i) it has the minimum power of Γ *and (2) it has the maximum value of p, especially in the cases of large values of* $|\Gamma| = |V_c - E|$.

4.2 Stability analysis

The stability analysis is based on the test problem:

$$q'' = -\omega^2 \, q. \tag{39}$$

where $\omega \neq \phi$, where ϕ is the frequency of the test problem (7) (phase–lag analysis) and ω is the frequency of the test problem (39) (stability analysis).

If we apply the new constructed pair (16) to the test problem (39) we obtained the difference equation:

$$\Omega_1(s,v)\ (q_{n+1}+q_{n-1})+\Omega_0(s,v)\ q_n=0 \tag{40}$$

and the corresponding characteristic equation:

$$\Omega_1(s,v)\ \left(\lambda^2+1\right)+\Omega_0(s,v)\ \lambda\ =\ 0 \tag{41}$$

withy the stability polynomials $\Omega_j(s,v)$, $j=0,1$ to be given by:

$$\begin{aligned}\Omega_1(s,v) &= 1+b_1\,s^2+c_3\,b_1\,s^4+c_1\,c_3\,b_1\,s^6\\ \Omega_0(s,v) &= a_1+b_0\,s^2-c_2\,b_1\,s^4-c_0\,c_3\,b_1\,s^6\end{aligned} \tag{42}$$

where $s=\omega\,h$ and $v=\phi\,h$. The observation that some coefficients of (42) are dependent on v, leads to the conclusion that the formulae (42) have dependence on s and v, while the formulae (19) have dependence only on v.

Substitution of the coefficients b_j, $j\ =\ 0,1$ and c_3 from (17) and the coefficients a_1, $c_i\,i=0(1)2$ from (26) into the above stability polynomials leads to:

$$\begin{aligned}\Omega_1(s,v) &= -\frac{\Upsilon_{10}(s,v)}{\Upsilon_{11}(s,v)}\\ \Omega_0(s,v) &= -\frac{\Upsilon_{12}(s,v)}{\Upsilon_{13}(s,v)}\end{aligned} \tag{43}$$

where $\Upsilon_j(s,v)$, $j=10(1)13$ are given in the Appendix F.

Remark 7. *The defined in Section 2 terms of P–stability and singularly almost P–stability are corresponded with problems having frequency which satisfied the condition $\omega=\phi$.*

The method (16) has a non zero interval of periodicity if the roots of its characteristic equation (41) satisfy the following condition:

$$|\lambda_{1,2}|\leq 1 \tag{44}$$

4.2.1 Construction of $s-v$ domain for the new scheme

The development of the $s-v$ domain for the new scheme is based on the following flowchart.

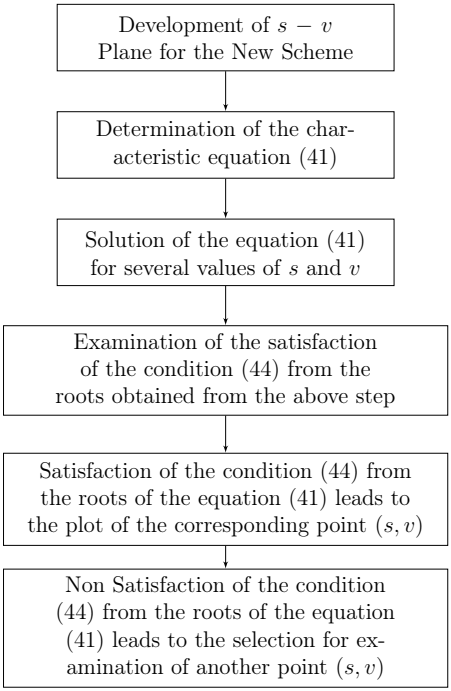

Figure 3. Flowchart for the development of $s - v$ domain for the new scheme

Based on the flowchart of the Figure 3, we produce the $s - v$ domain mentioned in Figure 4.

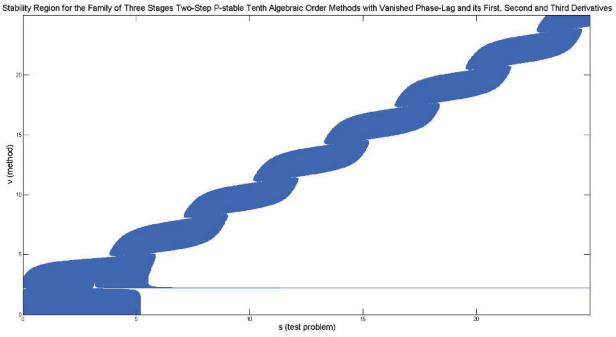

Figure 4. The plot of $s - v$ domain of the new developed P-stable two–stages pair with vanished phase–lag and its derivatives up to order three.

Remark 8. *The $s-v$ domain mentioned in the Figure 4 leads to the following observations:*

1. *The scheme is stable within the shadowed area of the domain.*
2. *The scheme is unstable within the white area of the domain.*

Remark 9. *The stability plane on $s-v$ domain of the scheme determines the categories of problems for which the specific scheme is appropriate:*

1. **Categories of problems for which** $\omega \neq \phi$. *For these categories of problems we have to give attention on all the plane of the $s-v$ domain* **excluding** *the plane around the first diagonal of the domain.*
2. **Categories of problems for which** $\omega = \phi$ *(see the Schrödinger equation and related problems). For these categories of problems we have to give attention on the plane around the first diagonal of the figure of the $s-v$ domain.*

The interval of periodicity of the new obtained scheme is defined as follows:

1. Substitution $s = v$ in the stability polynomials Ω_i, $i = 0, 1$ given by (43).
2. Observation of the plane around the first diagonal of the $s-v$ domain given in Figure 4.

The above leads to the computation of the interval of periodicity of the new obtained algorithm which is equal to $(0, \infty)$.

Remark 10. *The interval of periodicity is a property corresponding to categories of problems for which $s = v$ (Schrödinger equation and related problems).*

The above achievements lead to the following theorem:

Theorem 4. *The method obtained in Section 3:*

- *is of three stages*
- *is of tenth algebraic order,*
- *has eliminated the phase–lag and its derivatives up to order three and*
- *has an interval of periodicity equals to:* $(0, \infty)$ *i.e. is P–stable.*

5 Numerical results

In order to evaluate the efficiency of the new obtained scheme, we apply it to (1) the approximate solution of the radial time–independent Schrödinger equation and (2) the approximate solution of coupled differential equations arising from the Schrödinger equation.

5.1 Radial time–independent Schrödinger equation

The radial time–independent Schrödinger equation has the following model:

$$q''(r) = [l(l+1)/r^2 + V(r) - k^2]\, q(r), \tag{45}$$

where

1. The function $\Theta(r) = l(l+1)/r^2 + V(r)$ denotes *the effective potential* which satisfies the following property : $\Theta(r) \to 0$ as $r \to \infty$.
2. $k^2 \in \mathbb{R}$ denotes *the energy.*
3. $l \in \mathbb{Z}$ denotes *the angular momentum.*
4. The function V denotes *the potential.*

The problem (45) is a boundary value problem and consequently we need the determination of the boundary conditions which are given by:

$$q(0) = 0$$

and the boundary condition at the end point of integration domain which is determined for large values of r from the physical considerations of the specific problem.

Since the new obtained scheme is belonged to the frequency dependent methods (some of its coefficients are dependent from the $v = \phi\, h$), it is necessary the determination of the frequency ϕ, in order to be possible the new scheme to be applied to the numerical solution of the problem (45). For (45) and for the case $l = 0$ we have:

$$\phi = \sqrt{|V(r) - k^2|} = \sqrt{|V(r) - E|}$$

where $V(r)$ denotes the potential and $E = k^2$ denotes the energy.

5.1.1 Woods–Saxon potential

In order to solve numerically the problem (45), it is also necessary to determine the potential $V(r)$. For our numerical experiments we use the Wood–Saxon potential which is given by:

$$V(r) = \frac{\Psi_0}{1+\xi} - \frac{\Psi_0 \xi}{a(1+\xi)^2} \tag{46}$$

with $\xi = \exp\left[\frac{r-X_0}{a}\right]$, $\Psi_0 = -50$, $a = 0.6$, and $X_0 = 7.0$.

In Figure 5 we present the behavior of the Wood–Saxon potential for several values of r.

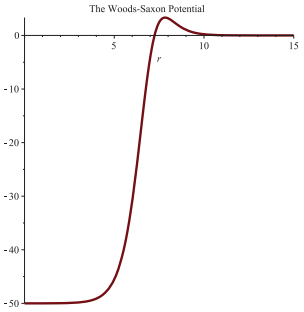

Figure 5. Behavior of the Woods–Saxon potential.

We determine the necessary value of the frequency ϕ as follows (see for details [18] and [19]):

$$\phi = \begin{cases} \sqrt{-50+E} & \text{for} \quad r \in [0, 6.5-2h] \\ \sqrt{-37.5+E} & \text{for} \quad r = 6.5-h \\ \sqrt{-25+E} & \text{for} \quad r = 6.5 \\ \sqrt{-12.5+E} & \text{for} \quad r = 6.5+h \\ \sqrt{E} & \text{for} \quad r \in [6.5+2h, 15]. \end{cases}$$

For the determination of the above mentioned values of the frequency ϕ we used the methodology introduced by Ixaru et al. ([17] and [19]). This methodology consists from discrete approximation of the continuous function $V(r)$ by constant values on some critical points within the integration area.

Here we give some examples from the determination of the values of ϕ:

1. On the point of the integration area $r = 6.5 - h$, the value of ϕ is equal to: $\sqrt{-37.5 + E}$. Consequently, $v = \phi\, h = \sqrt{-37.5 + E}\, h$.

2. On the point of the integration area $r = 6.5 - 3\, h$, the value of ϕ is equal to: $\sqrt{-50 + E}$. Consequently, $v = \phi\, h = \sqrt{-50 + E}\, h$.

We mention here that the potential $V(r)$ is a user defined function. In Chemistry there are many potentials which are of great interest. Very few potentials in Chemistry have known their eigenenergies. We selected the Woods–Saxon potential since for this potential the eigenenergies are known.

5.1.2 The resonance problem of the radial Schrödinger equation

The equation (45) is solved numerically with $l = 0$ and using the Woods-Saxon potential (46).

The problem mentioned above has an integration interval equal to $(0, \infty)$. Consequently, it is necessary to substitute the infinite interval of integration $(0, \infty)$ with a finite one. This approach leads to the numerical solution of the the above described problem. For our numerical experiments we request $r \in [0, 15]$. For our numerical tests we apply the numerical methods to be evaluated on a wide range of energies: $E \in [1, 1000]$.

Since for positive energies the potential $V(r)$ vanished faster than the term $\frac{l(l+1)}{r^2}$ for $r \to \infty$, the radial Schrödinger equation (45) can be expressed by the following model:

$$q''(r) + \left(k^2 - \frac{l(l+1)}{r^2}\right) q(r) = 0 \tag{47}$$

where the linearly independent solutions of the above model are given by $k\, r\, j_l(k\, r)$ and $k\, r\, n_l(k\, r)$, with $j_l(k\, r)$ and $n_l(k\, r)$ are the spherical Bessel and Neumann functions respectively (see [82]). Consequently, the asymptotic form of the solution of equation (45) (when $r \to \infty$) is given by:

$$\begin{aligned} q(r) &\approx A\, kr j_l(kr) - B\, kr n_l(kr) \\ &\approx AC\, \left[\sin\left(kr - \frac{l\pi}{2}\right) + \tan\delta_l \cos\left(kr - \frac{l\pi}{2}\right)\right] \end{aligned}$$

where δ_l is the phase shift and A, B, $AC \in \mathbb{R}$. The direct formula for the computation

of the phase shift is given by:

$$\tan \delta_l = \frac{q(r_2) S(r_1) - q(r_1) S(r_2)}{q(r_1) C(r_1) - q(r_2) C(r_2)}$$

where r_1 and r_2 are distinct points in the asymptotic region (we chosen $r_1 = 15$ and $r_2 = r_1 - h$) with $S(r) = k\, r\, j_l(k\, r)$ and $C(r) = -k\, r\, n_l(k\, r)$. Since the above mentioned problem is an initial–value one, the values of $q_j,\ j = 0, 1$ must be computed in order a two–step scheme to be applied. The value q_0 is defined by the initial condition of the problem. The value q_1 is computed using the high order Runge–Kutta–Nyström methods (see [20] and [21]). The computation of the values $q_i,\ i = 0, 1$ leads to the computation of the phase shift δ_l at the point r_2 of the asymptotic region. It is noted that q_j is the approximation of the function q at the point x_j.

Since the above mentioned problem is solved for positive energies, there are two possible outputs:

- the phase-shift δ_l or
- The energies E, for $E \in [1, 1000]$, for which $\delta_l = \frac{\pi}{2}$.

For our numerical tests the second problem is solved, which is known as **the resonance problem**.

The boundary conditions are:

$$q(0) = 0 \quad , \quad q(r) = \cos\left(\sqrt{E} r\right) \quad \text{for large } r.$$

The following methods are evaluated for the computation of the the positive eigenenergies of the resonance problem described above:

- **Method QT8**: the eighth order multi–step method developed by Quinlan and Tremaine [22];
- **Method QT10**: the tenth order multi–step method developed by Quinlan and Tremaine [22];
- **Method QT12**: the twelfth order multi–step method developed by Quinlan and Tremaine [22];
- **Method MCR4**: the fourth algebraic order method of Chawla and Rao with minimal phase–lag [23];

- **Method RA**: the exponentially–fitted method of Raptis and Allison [24];
- **Method MCR6**: the hybrid sixth algebraic order method developed by Chawla and Rao with minimal phase–lag [25];
- **Method NMPF1**: the Phase-Fitted Method (Case 1) developed in [12];
- **Method NMPF2**: the Phase-Fitted Method (Case 2) developed in [12];
- **Method NMC2**: the Method developed in [26] (Case 2);
- **Method NMC1**: the method developed in [26] (Case 1);
- **Method NM2SH2DV**: the Two-Step Hybrid Method developed in [1];
- **Method WPS2S**: the Two–Step P–stable Method developed in [81];
- **Method WPS4S**: the Four–Step P–stable Method developed in [81];
- **Method WPS6S**: the Six–Step P–stable Method developed in [81];
- **Method NM3SPS2DV**: the Three Stages Tenth Algebraic Order P–stable Symmetric Two–Step method with vanished phase-lag and its first and second derivatives developed in [6];
- **Method NM3SPS3DV**: the Three Stages Tenth Algebraic Order P–stable Symmetric Two–Step method with vanished phase-lag and its first, second and third derivatives developed in Section 3.

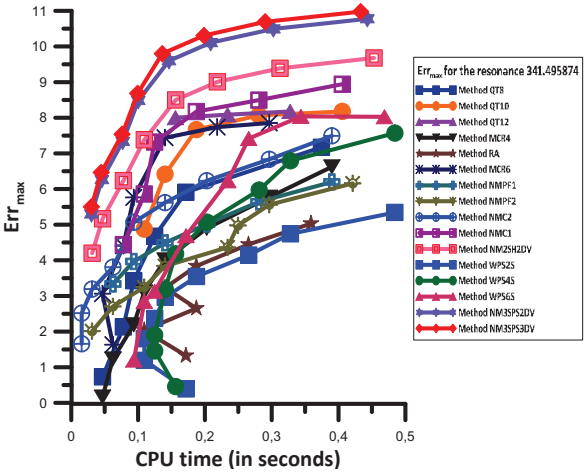

Figure 6. Accuracy (Digits) for several values of CPU Time (in Seconds) for the eigenvalue $E_2 = 341.495874$. The nonexistence of a value of Accuracy (Digits) indicates that for this value of CPU, Accuracy (Digits) is less than 0.

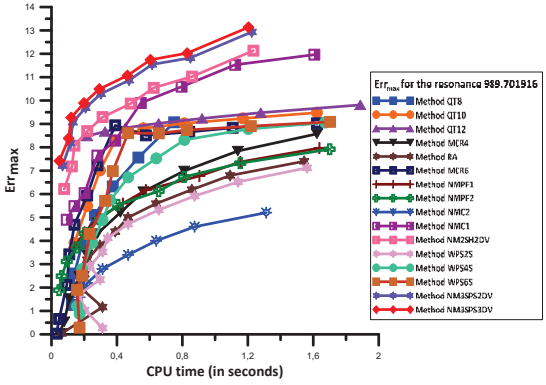

Figure 7. Accuracy (Digits) for several values of CPU Time (in Seconds) for the eigenvalue $E_3 = 989.701916$. The nonexistence of a value of Accuracy (Digits) indicates that for this value of CPU, Accuracy (Digits) is less than 0.

The maximum absolute error Err_{max} which is defined by: $Err_{max} = max|\log_{10}(Err)|$ where

$$Err = |E_{calculated} - E_{accurate}|$$

is presented in the Figures 6 and 7.

The absolute error Err is computed based on the calculated eigenenergies and the accurate eigenenergies (the reference values for the eigenenergies). The accurate eigenenergies are presented as $E_{accurate}$ and are computed using the well known two-step method of Chawla and Rao [25]. The calculated eigenenergies are presented as $E_{calculated}$ and are computed using each of the 16 numerical methods mentioned above.

In Figures 6 and 7 we present the maximum absolute errors Err_{max} for the eigenenergies $E_2 = 341.495874$ and $E_3 = 989.701916$, respectively, and for the 16 numerical methods mentioned above for several values of CPU time (in seconds). The denotations E_2 and E_3 for the calculated eigenenergies in our numerical example are given since it is known that the Woods–Saxon potential has also the eigenenergies E_0 and E_1. We chosen the eigenenergies E_2 and E_3 since for these values the solution has stiffer behavior and consequently the new obtained method can show its efficiency.

5.1.3 Conclusions on the obtained numerical results for the radial Schrödinger equation

The numerical results lead to the following conclusions:

- **Method QT10** is more efficient than **Method MCR4** and **Method QT8**.
- **Method QT10** is more efficient than **Method MCR6** for large CPU time and less efficient than **Method MCR6** for small CPU time.
- **Method QT12** is more efficient than **Method QT10**
- **Method NMPF1** is more efficient than **Method RA**, **Method NMPF2** and **Method WPS2S**
- **Method WPS4S** is more efficient than **Method MCR4**, **Method NMPF1** and **Method NMC2**.
- **Method WPS6S** is more efficient than **Method WPS4S**.
- **Method NMC1**, is more efficient than all the other methods mentioned above.
- **Method NM2SH2DV**, is more efficient than all the other methods mentioned above.

- **Method NM3SPS2DV**, is more efficient than all the other methods mentioned above.
- **Method NM3SPS3DV**, is the most efficient one.

5.2 Error estimation

We will use a so called variable–step pair in order to solve numerically the coupled differential equations of the Schrödinger form.

Definition 9. *A numerical pair is denoted of variable–step form if the step length of integration is changed during the integration process.*

Definition 10. *Local truncation error estimation (LTEE) is denoted the process which is used in order a variable–step pair to change the step length during the integration procedure.*

The last decades much research has been taken place on the construction of numerical pairs of constant or variable step length for the numerical solution of problems of the Schrödinger equation type (see for example [12]– [81]).

The numerical solution of the coupled Schrödinger equations is based on the variable–step pairs defined above. As also mentioned above the variable–step pairs are based on the LTEE procedure defined above. In Figure 8 the categories of LTEE procedures are presented.

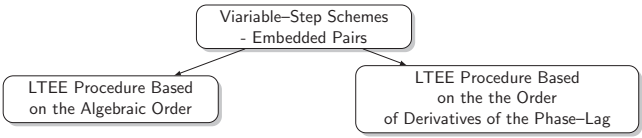

Figure 8. Categories of LTEE Procedures used for Developing Embedded Pairs for Problems with Oscillatory and/or Periodical solutions.

We use the following formula for the estimation of the local truncation error (LTE) in the lower order solution q_{n+1}^L:

$$LTE = \mid q_{n+1}^H - q_{n+1}^L \mid \tag{48}$$

where q_{n+1}^L and q_{n+1}^H are

- **LTEE Procedure based on the algebraic order of the pairs**. For this procedure, q_{n+1}^{L} denotes the scheme with the lower algebraic order solution and q_{n+1}^{H} denotes the scheme with the higher algebraic order solution.

- **LTEE Procedure based on the order of the derivatives of the phase–lag**. Consider that the higher order of the derivatives of the phase–lag which are vanished for the schemes which participate in this procedure are p and s respectively, where $p < s$. For this procedure q_{n+1}^{L} denotes the scheme with vanished higher order derivative of the phase–lag equal to p and q_{n+1}^{H} denotes the scheme with vanished higher order derivative of the phase–lag equal to s .

For our numerical tests we use the first LTEE procedure for the estimation of the local truncation error. Consequently, we use:

As q_{n+1}^{L} we use the eighth algebraic order method developed in [80] and as q_{n+1}^{H} we use the tenth algebraic order method developed in Section 3.

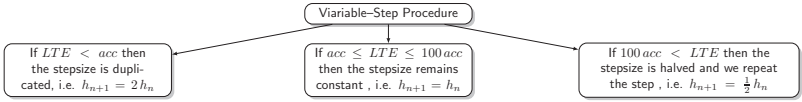

Figure 9. Variable–Step Procedure used in our Numerical Experiments.

The variable–step procedure which is used in our numerical tests is presented in Figure 9, where h_n is the stepsize which is used for the n^{th} step of the integration and acc is the accuracy of the local truncation error LTE which is denoted by the user.

Remark 11. *In our numerical experiments the known as* **local extrapolation** *technique is used. Based on this technique for the approximation at each point of the integration domain we use the higher order solution q_{n+1}^{H} although the local error estimation is based on the lower order solution q_{n+1}^{L}.*

5.3 Coupled differential equations of the Schrödinger type

The coupled Schrödinger equations can be occurred in many scientific disciplines like: quantum chemistry, material science, theoretical physics, quantum physics atomic physics, physical chemistry and chemical physics, quantum chemistry, etc.

The mathematical model of the close-coupling Schrödinger equations is given by:

$$\left[\frac{d^2}{dx^2} + k_i^2 - \frac{l_i(l_i+1)}{x^2} - V_{ii}\right] q_{ij} = \sum_{m=1}^{N} V_{im}\, q_{mj}$$

for $1 \leq i \leq N$ and $m \neq i$.

The above problem is a boundary value one and consequently the boundary conditions are given by (see for details [27]):

$$q_{ij} = 0 \; at \; x = 0$$

$$q_{ij} \sim k_i\, x j_{l_i}(k_i x)\delta_{ij} + \left(\frac{k_i}{k_j}\right)^{1/2} K_{ij}\, k_i\, x\, n_{li}(k_i x) \tag{49}$$

Remark 12. *The numerical pair obtained in this paper can be applied efficiently in both open and close channels problem.*

Based on the analysis described in [27], the new forms of the asymptotic condition is given by(49):

$$\mathbf{q} \sim \mathbf{M} + \mathbf{N}\mathbf{K}'.$$

where the matrix $\mathbf{K}'$ and diagonal matrices $\mathbf{M}$, $\mathbf{N}$ are give by :

$$\begin{aligned} K'_{ij} &= \left(\frac{k_i}{k_j}\right)^{1/2} K_{ij} \\ M_{ij} &= k_i x j_{l_i}(k_i x)\delta_{ij} \\ N_{ij} &= k_i x n_{l_i}(k_i x)\delta_{ij} \end{aligned}$$

The rotational excitation of a diatomic molecule by neutral particle impact is studied in this paper. In several scientific areas like quantum chemistry, theoretical chemistry, theoretical physics, quantum physics, material science, atomic physics, molecular physics, in technical applications in the analysis of gas dynamics and stratification of chemically reacting flows, dispersed flows, including with nano-sized particles etc this problem is occurred. The mathematical model of the above mentioned problem contains close–coupling Schrödinger equations (see [7], [8–11], [83] - [87]). Using the denotations:

- quantum numbers (j, l) which denote the entrance channel (see for details in [27]),
- quantum numbers (j', l') which denote the exit channels and
- $J = j + l = j' + l'$ which denote the total angular momentum.

we have:

$$\left[\frac{d^2}{dx^2}+k_{j'j}^2-\frac{l'(l'+1)}{x^2}\right]q_{j'l'}^{Jjl}(x)=\frac{2\mu}{\hbar^2}\sum_{j''}\sum_{l''}<j'l';J\mid V\mid j''l'';J>q_{j''l''}^{Jjl}(x)$$

where

$$k_{j'j}=\frac{2\mu}{\hbar^2}\left[E+\frac{\hbar^2}{2I}\{j(j+1)-j'(j'+1)\}\right].$$

and E denotes the kinetic energy of the incident particle in the center-of-mass system, I denotes the moment of inertia of the rotator, μ denotes the reduced mass of the system, Jjl is angular momentum of the quantum numbers (j,l) and j'' and l'' are quantum numbers.

We use the following potential V (see [27]) :

$$V(x,\hat{\mathbf{k}}_{j'j}\hat{\mathbf{k}}_{jj})=V_0(x)P_0(\hat{\mathbf{k}}_{j'j}\hat{\mathbf{k}}_{jj})+V_2(x)P_2(\hat{\mathbf{k}}_{j'j}\hat{\mathbf{k}}_{jj})$$

and therefore, the coupling matrix contains elements of the form:

$$<j'l';J\mid V\mid j''l'';J>=\delta_{j'j''}\delta_{l'l''}V_0(x)+f_2(j'l',j''l'';J)V_2(x)$$

where f_2 coefficients are denoted from formulae presented by Bernstein et al. [28] and $\hat{\mathbf{k}}_{j'j}$ is a unit vector parallel to the wave vector $\mathbf{k}_{j'j}$ and $P_i,\ i=0,2$ are Legendre polynomials (see for details [29]). We note also that $V_0(x)$ and $V_2(x)$ are potential functions and are defined by the user. The above leads to the following new expressions of the boundary conditions:

$$q_{j'l'}^{Jjl}(x)=0 \text{ at } x=0 \tag{50}$$

$$q_{j'l'}^{Jjl}(x)\sim\delta_{jj'}\delta_{ll'}\exp[-i(k_{jj}x-1/2l\pi)]-\left(\frac{k_i}{k_j}\right)^{1/2}S^J(jl;j'l')\exp[i(k_{j'j}x-1/2l'\pi)]$$

where S matrix. For K matrix of (49) we use the following formula:

$$\mathbf{S}=(\mathbf{I}+\mathbf{iK})(\mathbf{I}-\mathbf{iK})^{-1}.$$

For the numerical solution of the above described problem we follow the procedure fully described in [27]. The procedure contains the numerical scheme obtained in this paper for the integration from the initial value point to the matching points.

For our numerical experiments the following parameters for the **S** matrix are used:

$$\frac{2\mu}{\hbar^2}=1000.0\quad;\quad\frac{\mu}{I}=2.351\quad;\quad E=1.1$$

$$V_0(x)=\frac{1}{x^{12}}-2\frac{1}{x^6}\quad;\quad V_2(x)=0.2283V_0(x).$$

For our numerical experiments we chose (see for full details in [27]) $J = 6$ and for the excitation of the rotator the value $j = 0$ state to levels up to $j' = 2, 4$ and 6. The above values of the parameters define sets of **four, nine and sixteen coupled Schrödinger equations**, respectively. Based on the theory described in [29] and [27], the potential is considered infinite for x less than x_0. Therefore, the boundary condition (50) is written now as

$$q^{Jjl}_{j'l'}(x_0) = 0.$$

For the numerical solution of the above problem, we use the following methods:

- the Iterative Numerov method of Allison [27] which is indicated as **Method I**[2],
- the variable–step method of Raptis and Cash [30] which is indicated as **Method II**,
- the embedded Runge–Kutta Dormand and Prince method 5(4) (5(4) means: Runge–Kutta method of variable step which uses the fourth algebraic order part in order to control the error of the the fifth algebraic order part) which is developed in [21] which is indicated as **Method III**,
- the embedded Runge–Kutta method ERK4(2) developed in Simos [31] which is indicated as **Method IV**,
- the embedded two–step method developed in [1] which is indicated as **Method V**,
- the embedded two–step method developed in [2] which is indicated as **Method VI**.
- the embedded two–step method developed in [3] which is indicated as **Method VII**.
- the new developed embedded two–step method with error control based on the algebraic order of the method developed in [6] which is indicated as **Method VIII**.
- the new developed embedded two–step method with error control based on the algebraic order of the method developed in this paper which is indicated as **Method IX**.

In Table 2 we present the real time of computation requested by the numerical methods I-X mentioned above in order to calculate the square of the modulus of the **S** matrix for

[2]We note here that Iterative Numerov method developed by Allison [27] is one of the most well-known methods for the numerical solution of the coupled differential equations arising from the Schrödinger equation

the sets of 4, 9 and 16 coupled differential equations respectively. In the same table we also present the maximum error in the calculation of the square of the modulus of the **S** matrix.

All computations were carried out on a x86-64 compatible PC using double-precision arithmetic data type (64 bits) according to IEEE© Standard 754 for double precision.

6 Conclusions

A new P–stable symmetric two–step method with vanished phase–lag and its derivatives up to order three was developed in this paper. The construction of the new method was done on two stages:

1. In the first stage we satisfied the P–stability conditions introduced by Lambert and Watson [13] and Wang [81]

2. In the second stage, we satisfied the condition for the vanishing of the phase–lag.

3. In the third stage, we satisfied the conditions for the vanishing of the derivatives of the phase–lag.

We note here that the above methodology was first introduced in the paper of Medvedev and Simos [6].

We studied the new obtained method based on the following stages:

- We studied the determination of the local truncation error (LTE)

- We investigated the asymptotic form of the LTE and we compared the asymptotic form of the LTE of new pair with the asymptotic forms of the LTE of similar methods.

- We investigated the stability and the interval of periodicity properties of the new obtained scheme.

- We studied the computational efficiency of the new produced method.

The theoretical, computational and numerical achievements of this paper, proved the efficiency of the new obtained scheme compared with other well known and recently developed algorithms of the literature for the approximate solution of the radial Schrödinger equation and of the coupled Schrödinger equations.

Table 1. Coupled Differential Equations. Real time of computation (in seconds) (RTC) and maximum absolute error (MErr) to calculate $|S|^2$ for the variable–step methods Method I - Method VIII. acc=10^{-6}. Note that hmax is the maximum stepsize. N indicates the number of equations of the set of coupled differential equations

Method	N	hmax	RTC	MErr
Method I	4	0.014	3.25	1.2×10^{-3}
	9	0.014	23.51	5.7×10^{-2}
	16	0.014	99.15	6.8×10^{-1}
Method II	4	0.056	1.55	8.9×10^{-4}
	9	0.056	8.43	7.4×10^{-3}
	16	0.056	43.32	8.6×10^{-2}
Method III	4	0.007	45.15	9.0×10^{0}
	9			
	16			
Method IV	4	0.112	0.39	1.1×10^{-5}
	9	0.112	3.48	2.8×10^{-4}
	16	0.112	19.31	1.3×10^{-3}
Method V	4	0.448	0.20	1.1×10^{-6}
	9	0.448	2.07	5.7×10^{-6}
	16	0.448	11.18	8.7×10^{-6}
Method VI	4	0.448	0.15	3.2×10^{-7}
	9	0.448	1.40	4.3×10^{-7}
	16	0.448	10.13	5.6×10^{-7}
Method VII	4	0.448	0.10	2.5×10^{-7}
	9	0.448	1.10	3.9×10^{-7}
	16	0.448	9.43	4.2×10^{-7}
Method VIII	4	0.896	0.04	3.8×10^{-8}
	9	0.896	0.55	5.6×10^{-8}
	16	0.896	8.45	6.5×10^{-8}
Method IX	4	0.896	0.03	3.2×10^{-8}
	9	0.896	0.50	4.1×10^{-8}
	16	0.896	8.35	5.0×10^{-8}

Appendix A: Formulae for the $\Upsilon_i(v)$, $i = 2(1)5$

$$
\begin{aligned}
\Upsilon_2(v) &= 2\cos(v)\,v^6c_1 - v^6c_0 + 2\cos(v)\,v^4 - 30\,v^4c_2 \\
&+ 60\cos(v)\,v^2 + 300\,v^2 + 720\cos(v) + 360\,a_1 \\
\Upsilon_3(v) &= -\sin(v)\,v^{12}{c_1}^2 - 2\sin(v)\,v^{10}c_1 \\
&+ 30\,v^9c_1c_2 - 60\sin(v)\,v^8c_1 - v^9c_0 - \sin(v)\,v^8 \\
&- 720\sin(v)\,v^6c_1 - 60\,v^7c_0 - 600\,v^7c_1 - 60\sin(v)\,v^6 - 1080\,v^5a_1c_1 \\
&- 1080\,v^5c_0 - 900\,v^5c_2 - 1620\sin(v)\,v^4 - 300\,v^5 - 720\,v^3a_1 - 21600\,v^3c_2 \\
&- 21600\sin(v)\,v^2 - 10800\,va_1 - 129600\sin(v) + 108000\,v \\
\Upsilon_4(v) &= 38880000 + 7560\,v^{10}c_0c_1 - 2700000\,v^6c_1 - 1944000\,v^4c_0 \\
&- 23328000\,v^2c_2 - 183600\,v^6c_0 - 972000\,v^4c_2 - \cos(v)\,v^{12} + 10800\,v^{10}c_1c_2 \\
&+ 9720\,v^8a_1c_1 + 86400\,v^6a_1c_1 - v^{12}c_0 - 90\,v^{10}c_0 \\
&+ 2700\,v^{10}c_1 - 54000\,v^8c_1 + 3600\,v^6a_1 + 97200\,v^4a_1 - 5400\,v^8c_0 \\
&+ 2700\,v^8c_2 + 81000\,v^6c_2 + 194400\,v^2a_1 - 91800\cos(v)\,v^6 + 3000\,v^{12}{c_1}^2 \\
&- 1360800\cos(v)\,v^4 - 11664000\cos(v)\,v^2 + 7560\,v^{10}a_1{c_1}^2 - 46656000\cos(v) \\
&- 1296000\,v^4 - 9720000\,v^2 - 9000\,v^6 - 3888000\,a_1 - 90\cos(v)\,v^{10} \\
&- 3780\cos(v)\,v^8 + 30\,v^{12}c_1c_2 + 3\,v^{14}c_0c_1 + 300\,v^{12}c_0c_1 \\
&- 64800\cos(v)\,v^8c_1 - 90\,v^{14}{c_1}^2c_2 - 90\cos(v)\,v^{14}{c_1}^2 - 3\cos(v)\,v^{14}c_1 \\
&- 180\cos(v)\,v^{12}c_1 - 4860\cos(v)\,v^{10}c_1 - 1080\cos(v)\,v^{12}{c_1}^2 \\
&- 3\cos(v)\,v^{16}{c_1}^2 - 388800\cos(v)\,v^6c_1 \\
&+ 900\,v^8 - \cos(v)\,v^{18}{c_1}^3 - 1944000\,v^4a_1c_1 + 291600\,v^8c_1c_2 \\
\Upsilon_5(v) &= -13996800000\,v - 21600\,v^{15}{c_1}^2 + 1080000\,v^{13}{c_1}^2 - 14400\,v^{13}c_1 \\
&+ 6480\,v^{11}c_0 + 648000\,v^{11}c_1 - 21600\,v^9a_1 + 453600\,v^9c_0 - 777600\,v^7a_1 \\
&+ 6840\sin(v)\,v^{12} + 163296000\,v^3a_1 + \sin(v)\,v^{16} + 120\sin(v)\,v^{14} \\
&- 18000\,v^{17}{c_1}^3 - 1166400000\,v^3 - 43200\,v^{13}c_1c_2 - 129600\,v^{11}a_1{c_1}^2 \\
&- 82080\,v^{11}a_1c_1 - 712800\,v^{11}c_1c_2 + 4406400\,v^{11}c_0c_1 \\
&+ 54432000\,v^9a_1{c_1}^2 - 1296000\,v^9a_1c_1 + 54432000\,v^9c_0c_1 \\
&+ 40435200\,v^7a_1c_1 + 1213056000\,v^7c_1c_2 + \sin(v)\,v^{24}{c_1}^4 \\
&+ 4\sin(v)\,v^{22}{c_1}^3 + 120\sin(v)\,v^{20}{c_1}^3 \\
&+ 6\sin(v)\,v^{20}{c_1}^2 + 1440\sin(v)\,v^{18}{c_1}^3
\end{aligned}
$$

$$
\begin{aligned}
&+ \; 360\,\sin(v)\,v^{18}{c_1}^2 + 4\,\sin(v)\,v^{18}c_1 \\
&+ \; 9720\,\sin(v)\,v^{16}{c_1}^2 + 367200\,\sin(v)\,v^{12}c_1 \\
&+ \; 360\,\sin(v)\,v^{16}c_1 + 129600\,\sin(v)\,v^{14}{c_1}^2 + 15120\,\sin(v)\,v^{14}c_1 \\
&+ \; 360\,v^{19}{c_1}^3c_2 + 69984000\,v^9c_1c_2 + 16796160000\,\sin(v) \\
&+ \; 777600\,\sin(v)\,v^{12}{c_1}^2 + 373248000\,v^5a_1c_1 + 46656000\,\sin(v)\,v^8c_1 \\
&- \; 10800\,v^{11}c_2 + 40824000\,v^9c_1 - 324000\,v^9c_2 + 15552000\,v^7c_2 \\
&+ \; 5443200\,\sin(v)\,v^{10}c_1 - 2799360000\,v^3a_1c_1 - 12\,v^{19}c_0{c_1}^2 \\
&+ \; 237600\,\sin(v)\,v^{10} - 2799360000\,v^3c_0 - 16796160000\,vc_2 \\
&- \; 112320\,v^{13}a_1{c_1}^2 - 3369600\,v^{13}{c_1}^2c_2 + 108000\,v^{13}c_0c_1 + 12\,v^{17}c_0c_1 \\
&- \; 60480\,v^{15}c_0{c_1}^2 + 1440\,v^{15}c_0c_1 - 108000\,v^{15}{c_1}^2c_2 \\
&- \; 1800\,v^{17}c_0{c_1}^2 - 60480\,v^{15}a_1{c_1}^3 - 360\,v^{17}{c_1}^2c_2 \\
&- \; 279936000\,v^5c_0 + 886464000\,\sin(v)\,v^4 + 1399680000\,v^3c_2 \\
&+ \; 5598720000\,\sin(v)\,v^2 + 5475600\,\sin(v)\,v^8 \\
&+ \; 85536000\,\sin(v)\,v^6 - 6531840000\,v^5c_1 + 466560000\,v^5c_2 \\
&+ \; 839808000\,va_1 + 12960000\,v^7 + 108000\,v^9 - 3600\,v^{11} + 155520000\,v^5 \\
&+ \; 186624000\,\sin(v)\,v^6c_1 + 45360000\,v^{11}{c_1}^2.
\end{aligned}
$$

Appendix B: Formulae for the $\Upsilon_j(v)$, $j = 6(1)9$

$$
\begin{aligned}
\Upsilon_6(v) &= -(\cos(v))^2 v^7 - 63\,v^5(\cos(v))^2 \\
&- \; 2\,v^7 + 240\,v^4\sin(v)\cos(v) - 600\,\sin(v)\,v^4 \\
&- \; 1260\,(\cos(v))^2 v^3 - 117\,v^5 + 10440\,\sin(v)\cos(v)\,v^2 \\
&+ \; 5400\,\cos(v)\,v^3 + 9000\,\sin(v)\,v^2 \\
&+ \; 5400\,(\cos(v))^2 v - 900\,v^3 + 90720\,\sin(v)\cos(v) + 42120\,v \\
\Upsilon_7(v) &= (\cos(v))^2 v^7 + 12\,\sin(v)\cos(v)\,v^6 \\
&+ \; 15\,v^5(\cos(v))^2 + 2\,v^7 + 450\,v^4\sin(v)\cos(v) \\
&- \; 300\,\sin(v)\,v^4 + 540\,(\cos(v))^2 v^3 + 195\,v^5 \\
&+ \; 6480\,\sin(v)\cos(v)\,v^2 + 4500\,\cos(v)\,v^3 \\
&+ \; 17100\,\sin(v)\,v^2 + 17640\,(\cos(v))^2 v + 3420\,v^3 \\
&+ \; 32400\,\sin(v)\cos(v) - 14400\,\cos(v)\,v - 35640\,v
\end{aligned}
$$

$$
\begin{aligned}
\Upsilon_8(v) &= \sin(v)\,v^6 - 5\cos(v)\,v^5 + 35\sin(v)\,v^4 \\
&+ 30\cos(v)\,v^3 + 570\sin(v)\,v^2 + 3000\cos(v)\,v \\
&- 5400\sin(v) + 2400\,v \\
\Upsilon_9(v) &= (\cos(v))^2\,v^6 + 8\,v^5\sin(v)\cos(v) \\
&+ 55\,v^4(\cos(v))^2 + 2\,v^6 + 324\,v^3\sin(v)\cos(v) \\
&- 600\,v^3\sin(v) + 2220\,(\cos(v))^2\,v^2 + 169\,v^4 \\
&+ 4200\sin(v)\cos(v)\,v + 7800\cos(v)\,v^2 \\
&+ 21000\sin(v)\,v + 37800\,(\cos(v))^2 + 2580\,v^2 - 37800.
\end{aligned}
$$

Appendix C: Truncated Taylor Series Expansion Formulae for the coefficients of the new obtained method given by (26)

$$
\begin{aligned}
a_1 &= -2 + \frac{v^{12}}{47900160} + \frac{443\,v^{14}}{326918592000} \\
&+ \frac{5963\,v^{16}}{31384184832000} + \frac{223579\,v^{18}}{9146248151040000} + \cdots \\
c_0 &= \frac{15}{28} - \frac{v^4}{7392} + \frac{1241\,v^6}{32432400} + \frac{23563\,v^8}{7264857600} \\
&+ \frac{1858313\,v^{10}}{4234374144000} + \frac{2313033839\,v^{12}}{40548366802944000} \\
&+ \frac{310335550439\,v^{14}}{41629656584355840000} + \frac{22396738087177\,v^{16}}{22979570434564423680000} \\
&+ \frac{13705907211935027\,v^{18}}{10754438963376150282240000} + \cdots \\
c_1 &= \frac{1}{56} - \frac{v^4}{14784} - \frac{709\,v^6}{64864800} - \frac{181\,v^8}{121080960} \\
&- \frac{433747\,v^{10}}{2195601408000} - \frac{190939403\,v^{12}}{7372430327808000} \\
&- \frac{846454904003\,v^{14}}{249777939506135040000} - \frac{61108949840333\,v^{16}}{13787742260738654208000} \\
&- \frac{1133311624662463\,v^{18}}{19553525387956636876800000} + \cdots
\end{aligned}
$$

Appendix D: Expressions for the Derivatives of q_n

Expressions of the derivatives which are presented in the formulae of the Local Truncation Errors:

$$
\begin{aligned}
q^{(2)} &= (V(x) - V_c + \Gamma)\ q(x) \\
q^{(3)} &= \left(\frac{d}{dx}\Xi(x)\right) q(x) + (\Xi(x) + \Gamma)\frac{d}{dx}q(x) \\
q^{(4)} &= \left(\frac{d^2}{dx^2}\Xi(x)\right) q(x) + 2\left(\frac{d}{dx}\Xi(x)\right)\frac{d}{dx}q(x) + (\Xi(x) + \Gamma)^2 q(x) \\
q^{(5)} &= \left(\frac{d^3}{dx^3}\Xi(x)\right) q(x) + 3\left(\frac{d^2}{dx^2}\Xi(x)\right)\frac{d}{dx}q(x) \\
&+ 4(\Xi(x) + \Gamma) q(x)\frac{d}{dx}\Xi(x) + (\Xi(x) + \Gamma)^2\frac{d}{dx}q(x) \\
q^{(6)} &= \left(\frac{d^4}{dx^4}\Xi(x)\right) q(x) + 4\left(\frac{d^3}{dx^3}\Xi(x)\right)\frac{d}{dx}q(x) \\
&+ 7(\Xi(x) + \Gamma) q(x)\frac{d^2}{dx^2}\Xi(x) + 4\left(\frac{d}{dx}\Xi(x)\right)^2 q(x) \\
&+ 6(\Xi(x) + \Gamma)\left(\frac{d}{dx}q(x)\right)\frac{d}{dx}\Xi(x) + (\Xi(x) + \Gamma)^3 q(x) \\
q^{(7)} &= \left(\frac{d^5}{dx^5}\Xi(x)\right) q(x) + 5\left(\frac{d^4}{dx^4}\Xi(x)\right)\frac{d}{dx}q(x) \\
&+ 11(\Xi(x) + \Gamma) q(x)\frac{d^3}{dx^3}\Xi(x) + 15\left(\frac{d}{dx}\Xi(x)\right) q(x) \\
&+ \frac{d^2}{dx^2}\Xi(x) + 13\ (\Xi(x) + \Gamma)\left(\frac{d}{dx}q(x)\right)\frac{d^2}{dx^2}\Xi(x) \\
&+ 10\left(\frac{d}{dx}\Xi(x)\right)^2\frac{d}{dx}q(x) + 9\ (\Xi(x) + \Gamma)^2 q(x) \\
&+ \frac{d}{dx}\Xi(x) + (\Xi(x) + \Gamma)^3\frac{d}{dx}q(x) \\
q^{(8)} &= \left(\frac{d^6}{dx^6}\Xi(x)\right) q(x) + 6\left(\frac{d^5}{dx^5}\Xi(x)\right)\frac{d}{dx}q(x)
\end{aligned}
$$

$$
\begin{aligned}
&+ \quad 16\left(\Xi(x)+\Gamma\right)q(x)\frac{d^4}{dx^4}\Xi(x)+26\left(\frac{d}{dx}\Xi(x)\right)q(x)\\
&+ \quad \frac{d^3}{dx^3}\Xi(x)+24\left(\Xi(x)+\Gamma\right)\left(\frac{d}{dx}q(x)\right)\frac{d^3}{dx^3}\Xi(x)\\
&+ \quad 15\left(\frac{d^2}{dx^2}\Xi(x)\right)^2q(x)+48\left(\frac{d}{dx}\Xi(x)\right)\\
&+ \quad \left(\frac{d}{dx}q(x)\right)\frac{d^2}{dx^2}\Xi(x)+22\left(\Xi(x)+\Gamma\right)^2q(x)\\
&+ \quad \frac{d^2}{dx^2}\Xi(x)+28\left(\Xi(x)+\Gamma\right)q(x)\left(\frac{d}{dx}\Xi(x)\right)^2\\
&+ \quad 12\left(\Xi(x)+\Gamma\right)^2\left(\frac{d}{dx}q(x)\right)\frac{d}{dx}\Xi(x)+\left(\Xi(x)+\Gamma\right)^4q(x)\\
&\ldots
\end{aligned}
$$

We compute the j-th derivative of the function z at the point x_n, i.e. $z_n^{(j)}$, substituting in the above formulae x with x_n.

Appendix E: Formula for the quantity Λ_0

$$
\begin{aligned}
\Lambda_0 \;=\; & -\frac{743\,\Xi(x)\,q(x)\left(\frac{\mathrm{d}}{\mathrm{d}x}\Xi(x)\right)^2\frac{\mathrm{d}^2}{\mathrm{d}x^2}\Xi(x)}{5987520}-\frac{5\left(\Xi(x)\right)^2\left(\frac{\mathrm{d}}{\mathrm{d}x}q(x)\right)\left(\frac{\mathrm{d}}{\mathrm{d}x}\Xi(x)\right)\frac{\mathrm{d}^2}{\mathrm{d}x^2}\Xi(x)}{99792}\\
& -\frac{313\left(\Xi(x)\right)^2q(x)\left(\frac{\mathrm{d}}{\mathrm{d}x}\Xi(x)\right)\frac{\mathrm{d}^3}{\mathrm{d}x^3}\Xi(x)}{3991680}-\frac{23\,\Xi(x)\left(\frac{\mathrm{d}}{\mathrm{d}x}q(x)\right)\left(\frac{\mathrm{d}^4}{\mathrm{d}x^4}\Xi(x)\right)\frac{\mathrm{d}}{\mathrm{d}x}\Xi(x)}{299376}\\
& -\frac{19\left(\Xi(x)\right)^4q(x)\frac{\mathrm{d}^2}{\mathrm{d}x^2}\Xi(x)}{4790016}-\frac{5\left(\frac{\mathrm{d}^2}{\mathrm{d}x^2}\Xi(x)\right)^3q(x)}{177408}\\
& -\frac{\left(\frac{\mathrm{d}^4}{\mathrm{d}x^4}\Xi(x)\right)^2q(x)}{114048}-\frac{\left(\Xi(x)\right)^6q(x)}{23950080}-\frac{37\left(\Xi(x)\right)^3q(x)\frac{\mathrm{d}^4}{\mathrm{d}x^4}\Xi(x)}{2993760}\\
& -\frac{353\left(\frac{\mathrm{d}}{\mathrm{d}x}\Xi(x)\right)q(x)\left(\frac{\mathrm{d}^3}{\mathrm{d}x^3}\Xi(x)\right)\frac{\mathrm{d}^2}{\mathrm{d}x^2}\Xi(x)}{2395008}-\frac{323\,\Xi(x)\,q(x)\left(\frac{\mathrm{d}^5}{\mathrm{d}x^5}\Xi(x)\right)\frac{\mathrm{d}}{\mathrm{d}x}\Xi(x)}{5987520}\\
& -\frac{13\,\Xi(x)\,q(x)\left(\frac{\mathrm{d}^4}{\mathrm{d}x^4}\Xi(x)\right)\frac{\mathrm{d}^2}{\mathrm{d}x^2}\Xi(x)}{136080}-\frac{73\,\Xi(x)\left(\frac{\mathrm{d}}{\mathrm{d}x}q(x)\right)\left(\frac{\mathrm{d}^3}{\mathrm{d}x^3}\Xi(x)\right)\frac{\mathrm{d}^2}{\mathrm{d}x^2}\Xi(x)}{598752}\\
& -\frac{\left(\frac{\mathrm{d}}{\mathrm{d}x}\Xi(x)\right)^4q(x)}{85536}-\frac{157\left(\Xi(x)\right)^2\left(\frac{\mathrm{d}}{\mathrm{d}x}q(x)\right)\frac{\mathrm{d}^5}{\mathrm{d}x^5}\Xi(x)}{11975040}
\end{aligned}
$$

$$
\begin{aligned}
&- \frac{17\left(\frac{\mathrm{d}^2}{\mathrm{d}x^2}\Xi(x)\right)q(x)\frac{\mathrm{d}^6}{\mathrm{d}x^6}\Xi(x)}{1596672} - \frac{13\left(\frac{\mathrm{d}}{\mathrm{d}x}\Xi(x)\right)q(x)\frac{\mathrm{d}^7}{\mathrm{d}x^7}\Xi(x)}{2395008} \\
&- \frac{7\left(\frac{\mathrm{d}}{\mathrm{d}x}\Xi(x)\right)\left(\frac{\mathrm{d}}{\mathrm{d}x}q(x)\right)\frac{\mathrm{d}^6}{\mathrm{d}x^6}\Xi(x)}{342144} - \frac{23\,\Xi(x)\,q(x)\frac{\mathrm{d}^8}{\mathrm{d}x^8}\Xi(x)}{11975040} \\
&- \frac{19\left(\frac{\mathrm{d}^2}{\mathrm{d}x^2}\Xi(x)\right)\left(\frac{\mathrm{d}}{\mathrm{d}x}q(x)\right)\frac{\mathrm{d}^5}{\mathrm{d}x^5}\Xi(x)}{443520} - \frac{31\left(\frac{\mathrm{d}}{\mathrm{d}x}\Xi(x)\right)\left(\frac{\mathrm{d}}{\mathrm{d}x}q(x)\right)\left(\frac{\mathrm{d}^2}{\mathrm{d}x^2}\Xi(x)\right)^2}{266112} \\
&- \frac{43\,\Xi(x)\,q(x)\left(\frac{\mathrm{d}^3}{\mathrm{d}x^3}\Xi(x)\right)^2}{748440} - \frac{(\Xi(x))^4\left(\frac{\mathrm{d}}{\mathrm{d}x}q(x)\right)\frac{\mathrm{d}}{\mathrm{d}x}\Xi(x)}{798336} \\
&- \frac{5\,\Xi(x)\left(\frac{\mathrm{d}}{\mathrm{d}x}q(x)\right)\left(\frac{\mathrm{d}}{\mathrm{d}x}\Xi(x)\right)^3}{199584} - \frac{239\,(\Xi(x))^2\,q(x)\frac{\mathrm{d}^6}{\mathrm{d}x^6}\Xi(x)}{23950080} \\
&- \frac{5\,(\Xi(x))^3\left(\frac{\mathrm{d}}{\mathrm{d}x}q(x)\right)\frac{\mathrm{d}^3}{\mathrm{d}x^3}\Xi(x)}{598752} - \frac{\Xi(x)\left(\frac{\mathrm{d}}{\mathrm{d}x}q(x)\right)\frac{\mathrm{d}^7}{\mathrm{d}x^7}\Xi(x)}{187110} \\
&- \frac{1201\,(\Xi(x))^2\,q(x)\left(\frac{\mathrm{d}^2}{\mathrm{d}x^2}\Xi(x)\right)^2}{23950080} - \frac{\left(\frac{\mathrm{d}^3}{\mathrm{d}x^3}\Xi(x)\right)\left(\frac{\mathrm{d}}{\mathrm{d}x}q(x)\right)\frac{\mathrm{d}^4}{\mathrm{d}x^4}\Xi(x)}{16632} \\
&- \frac{31\left(\frac{\mathrm{d}^3}{\mathrm{d}x^3}\Xi(x)\right)q(x)\frac{\mathrm{d}^5}{\mathrm{d}x^5}\Xi(x)}{1995840} - \frac{109\left(\frac{\mathrm{d}}{\mathrm{d}x}\Xi(x)\right)^2\left(\frac{\mathrm{d}}{\mathrm{d}x}q(x)\right)\frac{\mathrm{d}^3}{\mathrm{d}x^3}\Xi(x)}{1197504} \\
&- \frac{\left(\frac{\mathrm{d}}{\mathrm{d}x}\Xi(x)\right)^2 q(x)\frac{\mathrm{d}^4}{\mathrm{d}x^4}\Xi(x)}{19008} - \frac{13\,(\Xi(x))^3\,q(x)\left(\frac{\mathrm{d}}{\mathrm{d}x}\Xi(x)\right)^2}{1197504} \\
&- \frac{\left(\frac{\mathrm{d}^{10}}{\mathrm{d}x^{10}}\Xi(x)\right)q(x)}{23950080} - \frac{\left(\frac{\mathrm{d}^9}{\mathrm{d}x^9}\Xi(x)\right)\frac{\mathrm{d}}{\mathrm{d}x}q(x)}{2395008}
\end{aligned}
$$

at every point $x = x_n$.

Appendix F: Formulae for the $\Upsilon_j(v)$, $j = 10(1)13$

$$
\begin{aligned}
\Upsilon_{10}(s,v) &= \sin(v)\,s^6v^6 - \sin(v)\,s^4v^8 - 5\cos(v)\,s^6v^5 \\
&+ 11\cos(v)\,s^4v^7 + 35\sin(v)\,s^6v^4 + 21\sin(v)\,s^4v^6 - 30\sin(v)\,s^2v^8 \\
&+ 30\cos(v)\,s^6v^3 + 330\cos(v)\,s^2v^7 + 570\sin(v)\,s^6v^2 \\
&+ 630\sin(v)\,s^2v^6 - 360\sin(v)\,v^8 + 3000\cos(v)\,s^6v \\
&+ 3960\cos(v)\,v^7 - 5400\sin(v)\,s^6 + 7560\sin(v)\,v^6 + 2400\,s^6v \\
\Upsilon_{11}(s,v) &= 360\,v^6\left(\sin(v)\,v^2 - 11\cos(v)\,v - 21\sin(v)\right) \\
\Upsilon_{12}(s,v) &= 24\sin(v)\cos(v)\,s^6v^6 - 24\sin(v)\cos(v)\,s^4v^8 \\
&+ 900\sin(v)\cos(v)\,s^6v^4 - 972\sin(v)\cos(v)\,s^4v^6 \\
&+ 12960\sin(v)\cos(v)\,s^6v^2 - 12600\sin(v)\cos(v)\,s^4v^4 \\
&- 9000\sin(v)\,v^8 - 71280\,s^6v - 90720\sin(v)\cos(v)\,v^6 - 5400\,(\cos(v))^2\,v^7 \\
&+ (\cos(v))^2\,v^{13} - 6660\,(\cos(v))^2\,s^4v^5
\end{aligned}
$$

$$
\begin{aligned}
&+ \; 2\,(\cos(v))^2\, s^6 v^7 + 35280\,(\cos(v))^2\, s^6 v \\
&- \; 240\,\sin(v)\cos(v)\, v^{10} - 3\,(\cos(v))^2\, s^4 v^9 \\
&- \; 23400\,\cos(v)\, s^4 v^5 + 1080\,(\cos(v))^2\, s^6 v^3 \\
&- \; 28800\,\cos(v)\, s^6 v - 1800\,\sin(v)\, s^2 v^8 + 9000\,\cos(v)\, s^6 v^3 \\
&+ \; 19800\,\cos(v)\, s^2 v^7 + 1800\,\sin(v)\, s^4 v^6 + 37800\,\sin(v)\, s^2 v^6 \\
&+ \; 34200\,\sin(v)\, s^6 v^2 - 600\,\sin(v)\, s^6 v^4 \\
&- \; 165\,(\cos(v))^2\, s^4 v^7 - 10440\,\sin(v)\cos(v)\, v^8 \\
&+ \; 30\,(\cos(v))^2\, s^6 v^5 - 113400\,(\cos(v))^2\, s^4 v^3 \\
&+ \; 64800\,\sin(v)\cos(v)\, s^6 - 63000\,\sin(v)\, s^4 v^4 - 507\, s^4 v^7 \\
&- \; 7740\, s^4 v^5 + 113400\, s^4 v^3 - 6\, s^4 v^9 + 390\, s^6 v^5 + 6840\, s^6 v^3 + 63\,(\cos(v))^2\, v^{11} \\
&+ \; 600\,\sin(v)\, v^{10} + 1260\,(\cos(v))^2\, v^9 \\
&- \; 5400\,\cos(v)\, v^9 + 4\, s^6 v^7 + 900\, v^9 + 117\, v^{11} - 42120\, v^7 + 2\, v^{13} \\
\Upsilon_{13}(s,v) \;&= \; 2160\, v^6 \left(\sin(v)\, v^2 - 11\,\cos(v)\, v - 21\,\sin(v)\right).
\end{aligned}
$$

References

[1] F. Hui, T. E. Simos, Hybrid high algebraic order two–step method with vanished phase–lag and its first and second derivatives, *MATCH Commun. Math. Comput. Chem.* **73** (2015) 619–648.

[2] J. Ma, T. E. Simos, Runge–Kutta type tenth algebraic order two–step method with vanished phase–lag and its first, second and third derivatives, *MATCH Commun. Math. Comput. Chem.* **74** (2015) 609–644.

[3] Z. Zhou, T. E. Simos, Three–stages tenth algebraic order two–step method with vanished phase–lag and its first, second, third and fourth derivatives, *MATCH Commun. Math. Comput. Chem.* **75** (2015) 653–694.

[4] T. Lei, T. E. Simos, Four–stages twelfth algebraic order two–step method with vanished phase–lag and its first and second derivatives, for the numerical solution of the Schrödinger equation *MATCH Commun. Math. Comput. Chem.* **76** (2016) 475–510.

[5] T. Lei, T. E. Simos, A new four–stages high algebraic order two–step method with vanished phase–lag and its first, second and third derivatives for the numerical solution of the Schrödinger equation, *MATCH Commun. Math. Comput. Chem.* **77** (2017) 333–392.

[6] M. A. Medvedev, T. E. Simos, New High Order P-stable Method with Optimal Phase Properties, *MATCH Commun. Math. Comput. Chem.* accepted.

[7] R. Vujasin, M. Senčanski, J. Radić–Perić, M. Perić, A comparison of various variational approaches for solving the one–dimensional vibrational Schrödinger equation, *MATCH Commun. Math. Comput. Chem.* **63** (2010) 363–378.

[8] C. J. Cramer, *Essentials of Computational Chemistry*, Wiley, Chichester, 2004.

[9] F. Jensen, *Introduction to Computational Chemistry*, Wiley, Chichester, 2007.

[10] A. R. Leach, *Molecular Modelling — Principles and Applications*, Pearson, Essex, 2001.

[11] P. Atkins, R. Friedman, *Molecular Quantum Mechanics*, Oxford Univ. Press, Oxford, 2011.

[12] Z. A. Anastassi, T. E. Simos, A parametric symmetric linear four–step method for the efficient integration of the Schrödinger equation and related oscillatory problems, *J. Comp. Appl. Math.* **236** (2012) 3880–3889.

[13] J. D. Lambert, I. A. Watson, Symmetric multistep methods for periodic initial values problems, *J. Inst. Math. Appl.* **18** (1976) 189–202.

[14] T. E. Simos, P. S. Williams, A finite–difference method for the numerical solution of the Schrödinger equation, *J. Comp. Appl. Math.* **79** (1997) 189–205.

[15] R. M. Thomas, Phase properties of high order almost P-stable formulae, *BIT* **24** (1984) 225–238.

[16] A. D. Raptis, T. E. Simos, A four–step phase–fitted method for the numerical integration of second order initial–value problem, *BIT* **31** (1991) 160–168.

[17] L. G. Ixaru, M. Rizea, Comparison of some four–step methods for the numerical solution of the Schrödinger equation, *Comput. Phys. Commun.* **38** (1985) 329–337.

[18] L. G. Ixaru, M. Micu, *Topics in Theoretical Physics*, Central Inst. Phys., Bucharest, 1978.

[19] L. G. Ixaru, M. Rizea, A Numerov–like scheme for the numerical solution of the Schrödinger equation in the deep continuum spectrum of energies, *Comput. Phys. Commun.* **19** (1980) 23–27.

[20] J. R. Dormand, M. E. A. El–Mikkawy, P. J. Prince, Families of Runge–Kutta–Nyström formulae, *IMA J. Numer. Anal.* **7** (1987) 235–250.

[21] J. R. Dormand, P. J. Prince, A family of embedded Runge–Kutta formulae, *J. Comput. Appl. Math.* **6** (1980) 19–26.

[22] G. D. Quinlan, S. Tremaine, Symmetric multistep methods for the numerical integration of planetary orbits, *Astronom. J.* **100** (1990) 1694–1700.

[23] M. M. Chawla, P. S. Rao, An Noumerov–type method with minimal phase–lag for the integration of second order periodic initial–value problems. II. Explicit method, *J. Comput. Appl. Math.* **15** (1986) 329–337.

[24] A. D. Raptis, A. C. Allison, Exponential–fitting methods for the numerical solution of the Schrödinger equation, *Comput. Phys. Commun.* **14** (1978) 1–5.

[25] M. M. Chawla, P. S. Rao, An explicit sixth–order method with phase–lag of order eight for $y'' = f(t, y)$, *J. Comput. Appl. Math.* **17** (1987) 363—368.

[26] T. E. Simos, On the explicit four–step methods with vanished phase–lag and its first derivative, *Appl. Math. Inf. Sci.* **8** (2014) 447–458.

[27] A. C. Allison, The numerical solution of coupled differential equations arising from the Schrödinger equation, *J. Comput. Phys.* **6** (1970) 378–391.

[28] R. B. Bernstein, A. Dalgarno, H. Massey, I. C. Percival, Thermal scattering of atoms by homonuclear diatomic molecules, *Proc. Roy. Soc. Ser. A* **274** (1963) 427–442.

[29] R. B. Bernstein, Quantum mechanical (phase shift) analysis of differential elastic scattering of molecular beams, *J. Chem. Phys.* **33** (1960) 795–804.

[30] A. D. Raptis, J. R. Cash, A variable step method for the numerical integration of the one–dimensional Schrödinger equation, *Comput. Phys. Commun.* **36** (1985) 113–119.

[31] T. E. Simos, Exponentially fitted Runge–Kutta methods for the numerical solution of the Schrödinger equation and related problems, *Comput. Mater. Sci.* **18** (2000) 315–332.

[32] G. A. Panopoulos, T. E. Simos, A new optimized symmetric embedded predictor–corrector method (EPCM) for initial–value problems with oscillatory solutions, *Appl. Math. Inf. Sci.* **8** (2014) 703–713.

[33] J. M. Franco, M. Palacios, High–order P-stable multistep methods, *J. Comput. Appl. Math.* **30** (1990) 1–10.

[34] J. D.Lambert, *Numerical Methods for Ordinary Differential Systems. The Initial Value Problem*, Wiley, New York, 1991, pp. 104–107.

[35] E. Stiefel, D. G. Bettis, Stabilization of Cowell's method, *Numer. Math.* **13** (1969) 154–175.

[36] G. A. Panopoulos, Z. A. Anastassi, T. E. Simos, Two new optimized eight–step symmetric methods for the efficient solution of the Schrödinger equation and related problems, *MATCH Commun. Math. Comput. Chem.* **60** (2008) 773–785.

[37] T. E. Simos, G. Psihoyios, Preface, in: *Selected Papers of the International Conference on Computational Methods in Sciences and Engineering (ICCMSE 2003)*, *J. Comput. Appl. Math.* **175** (2005) IX–IX.

[38] T. Lyche, Chebyshevian multistep methods for ordinary differential eqations, *Numer. Math.* **19** (1972) 65–75.

[39] A. Konguetsof, T. E. Simos, A generator of hybrid symmetric four–step methods for the numerical solution of the Schrödinger equation, *J. Comput. Appl. Math.* **158** (2003) 93–106.

[40] Z. Kalogiratou, T. Monovasilis, T. E. Simos, Symplectic integrators for the numerical solution of the Schrödinger equation, *J. Comput. Appl. Math.* **158** (2003) 83–92.

[41] Z. Kalogiratou, T. E. Simos, Newton–Cotes formulae for long–time integration, *J. Comput. Appl. Math.* **158** (2003) 75–82.

[42] G. Psihoyios, T. E. Simos, Trigonometrically fitted predictor–corrector methods for IVPs with oscillating solutions, *J. Comput. Appl. Math.* **158** (2003) 135–144.

[43] T. E. Simos, I. T. Famelis, C. Tsitouras, Zero dissipative, explicit Numerov–type methods for second order IVPs with oscillating solutions, *Numer. Algor.* **34** (2003) 27–40.

[44] T. E. Simos, Dissipative trigonometrically–fitted methods for linear second–order IVPs with oscillating solution, *Appl. Math. Lett.* **17** (2004) 601–607.

[45] K. Tselios, T. E. Simos, Runge–Kutta methods with minimal dispersion and dissipation for problems arising from computational acoustics, *J. Comput. Appl. Math.* **175** (2005) 173–181.

[46] D. P. Sakas, T. E. Simos, Multiderivative methods of eighth algrebraic order with minimal phase–lag for the numerical solution of the radial Schrödinger equation, *J. Comput. Appl. Math.* **175** (2005) 161–172.

[47] G. Psihoyios, T. E. Simos, A fourth algebraic order trigonometrically fitted predictor–corrector scheme for IVPs with oscillating solutions, *J. Comput. Appl. Math.* **175** (2005) 137–147.

[48] Z. A. Anastassi, T. E. Simos, An optimized Runge–Kutta method for the solution of orbital problems, *J. Comput. Appl. Math.* **175** (2005) 1–9.

[49] T. E. Simos, Closed Newton–Cotes trigonometrically–fitted formulae of high order for long–time integration of orbital problems, *Appl. Math. Lett.* **22** (2009) 1616–1621.

[50] S. Stavroyiannis, T. E. Simos, Optimization as a function of the phase–lag order of nonlinear explicit two–step P-stable method for linear periodic IVPs, *Appl. Numer. Math.* **59** (2009) 2467–2474.

[51] T. E. Simos, Exponentially and trigonometrically fitted methods for the solution of the Schrödinger equation, *Acta Appl. Math.* **110** (2010) 1331–1352.

[52] T. E. Simos, New stable closed Newton–Cotes trigonometrically fitted formulae for long–time integration, *Abstract Appl. Anal.* (2012) #182536.

[53] T. E. Simos, Optimizing a hybrid two–step method for the numerical solution of the Schrödinger equation and related problems with respect to phase–lag, *J. Appl. Math.* (2012) #420387.

[54] D. F. Papadopoulos, T. E. Simos, A modified Runge–Kutta–Nyström method by using phase lag properties for the numerical solution of orbital problems, *Appl. Math. Inf. Sci.* **7** (2013) 433–437.

[55] T. Monovasilis, Z. Kalogiratou, T. E. Simos, Exponentially fitted symplectic Runge–Kutta–Nyström methods, *Appl. Math. Inf. Sci.* **7** (2013) 81–85.

[56] G. A. Panopoulos, T. E. Simos, An optimized symmetric 8-step semi–embedded predictor–corrector method for IVPs with oscillating solutions, *Appl. Math. Inf. Sci.* **7** (2013) 73–80.

[57] D. F. Papadopoulos, T. E. Simos, The use of phase lag and amplification error derivatives for the construction of a modified Runge–Kutta–Nyström method, *Abstract Appl. Anal.* (2013) #910624.

[58] I. Alolyan, Z. A. Anastassi, T. E. Simos, A new family of symmetric linear four–step methods for the efficient integration of the Schrödinger equation and related oscillatory problems, *Appl. Math. Comput.* **218** (2012) 5370–5382.

[59] I. Alolyan, T. E. Simos, A family of high–order multistep methods with vanished phase–lag and its derivatives for the numerical solution of the Schrödinger equation, *Comput. Math. Appl.* **62** (2011) 3756–3774.

[60] C. Tsitouras, I. T. Famelis, T. E. Simos, On modified Runge–Kutta trees and methods, *Comput. Math. Appl.* **62** (2011) 2101–2111.

[61] C. Tsitouras, I. T. Famelis, T. E. Simos, Phase-fitted Runge–Kutta pairs of orders 8(7), *J. Comp. Appl. Math.* **321** (2017) 226–231.

[62] T. E. Simos, C. Tsitouras, Evolutionary generation of high order, explicit two step methods for second order linear IVPs, *Math. Meth. Appl. Sci.*, in press.

[63] A. A. Kosti, Z. A. Anastassi, T. E. Simos, Construction of an optimized explicit Runge–Kutta–Nyström method for the numerical solution of oscillatory initial value problems, *Comput. Math. Appl.* **61** (2011) 3381–3390.

[64] Z. Kalogiratou, T. Monovasilis, T. E. Simos, New modified Runge–Kutta–Nyström methods for the numerical integration of the Schrödinger equation, *Comput. Math. Appl.* **60** (2010) 1639–1647.

[65] T. Monovasilis, Z. Kalogiratou, T. E. Simos, A family of trigonometrically fitted partitioned Runge–Kutta symplectic methods, *Appl. Math. Comput.* **209** (2009) 91–96.

[66] T. Monovasilis , Z. Kalogiratou, H. Ramos, T. E. Simos, Modified two-step hybrid methods for the numerical integration of oscillatory problems, *Math. Meth. Appl. Sci.*, in press.

[67] T. E. Simos, C. Tsitouras, I. T. Famelis, Review on explicit Numerov type methods with constant coefficients, *Appl. Comput. Math.*, in press.

[68] T. E. Simos, High order closed Newton–Cotes trigonometrically–fitted formulae for the numerical solution of the Schrödinger equation, *Appl. Math. Comput.* **209** (2009) 137–151.

[69] Th. E. Simos, Multistage symmetric two–step P–stable method with vanished phase–lag and its first, second and third derivatives, *Appl. Comput. Math.* **14** (2015) 296–315.

[70] F. Hui, T. E. Simos, Four stages symmetric two–step P–stable method with vanished phase-lag and its first, second, third and fourth derivatives, *Appl. Comput. Math.* **15** (2016) 220–238

[71] G. A. Panopoulos, T. E. Simos, An eight–step semi–embedded predictor–corrector method for orbital problems and related IVPs with oscillatory solutions for which the frequency is unknown, *J. Comp. Appl. Math.* **290** (2015) 1–15.

[72] H. Ramos, Z. Kalogiratou, T. Monovasilis, T. E. Simos, An optimized two–step hybrid block method for solving general second order initial–value problems, *Num. Alg.* **72** (2016) 1089–1102.

[73] Z. Kalogiratou, T. Monovasilis, H. Ramos, T. E. Simos, A new approach on the construction of trigonometrically fitted two step hybrid methods, *J. Comp. Appl. Math.* **303** (2016) 146–155.

[74] T. Monovasilis, Z. Kalogiratou, T. E. Simos, Construction of exponentially fitted symplectic Runge–Kutta–Nyström methods from partitioned Runge–Kutta methods, *Mediterr. J. Math.* **13** (2016) 2271–2285.

[75] A. Konguetsof, T. E. Simos, An exponentially–fitted and trigonometrically–fitted method for the numerical solution of periodic initial–value problems, *Comput. Math. Appl.* **45** (2003) 547–554.

[76] D. F. Papadopoulos, Z. A. Anastassi, T. E. Simos, An optimized Runge–Kutta–Nyström method for the numerical solution of the Schrödinger equation and related problems, *MATCH Commun. Math. Comput. Chem.* **64** (2010) 551–566.

[77] Z. A. Anastassi, T. E. Simos, Trigonometrically fitted six–step symmetric methods for the efficient solution of the Schrödinger equation, *MATCH Commun. Math. Comput. Chem.* **60** (2008) 733–752.

[78] W. Zhang and T. E. Simos, A high-order two-step phase-fitted method for the numerical solution of the Schrödinger equation, *Mediterr. J. Math.* **13** (2016) 5177–5194.

[79] M. Dong, T. E. Simos, A new high algebraic order efficient finite difference method for the solution of the Schrödinger equation, *Filomat*, in press.

[80] T. E. Simos, A new Numerov–type method for the numerical solution of the Schrödinger equation, *J. Math. Chem.* **46** (2009) 981–1007.

[81] Z. Wang, P–stable linear symmetric multistep methods for periodic initial–value problems, *Comput. Phys. Commun.* **171** (2005) 162–174.

[82] W. E. Boyce, R. D. DiPrima, *Elementary Differential Equations and Boundary Value Problems*, Wiley, New York, 1969.

[83] V. N. Kovalnogov, R. V. Fedorov, L. V. Khakhaleva, D. A. Generalov, A. V. Chukalin, Development and investigation of the technologies involving thermal protection of surfaces immersed in disperse working medium flow, *Int. J. Energy Clean Environ.* **17** (2016) 223-239.

[84] V. N. Kovalnogov, R. V. Fedorov, Numerical analysis of the efficiency of film cooling of surface streamlined by supersonic disperse flow, *AIP Conf. Proceed.* **1648** (2015) 850031.

[85] V. N. Kovalnogov, R. V. Fedorov, T. V. Karpukhina, E. V. Tsvetova, Numerical analysis of the temperature stratification of the disperse flow, *AIP Conf. Proceed.* **1648** (2015) 850033.

[86] N. Kovalnogov, E. Nadyseva, O. Shakhov, V. Kovalnogov, Control of turbulent transfer in the boundary layer through applied periodic effects, *Izvestiya Vysshikh Uchebnykh Zavedenii Aviatsionaya Tekhnika* **1** (1998) 49-53.

[87] N. Kovalnogov, V. Kovalnogov, Characteristics of numerical integration and conditions of solution stability in the system of differential equations of boundary layer, subjected to the intense influence, *Izvestiya Vysshikh Uchebnykh Zavedenii Aviatsionaya Tekhnika* **1** (1996) 58-61.

[88] S. Kottwitz, *LaTeX Cookbook*, Packt Pub., Birmingham, 2015, pp. 231–236.